

A general description of the “ALARO” concept and its realisation

R. Brožková

January 21, 2014

The description below shall not refer to any particular ALARO software concretisation. There exists since end of 2012 an “ALARO-0 baseline” and all our items will either correspond to it or to on-going evolutions targeted for first implementations in 2014. The latter are grouped under an ALARO-1 label. We shall neither refer to any particular IFS/ARPEGE library Cycle; corresponding details may be provided rather independently, if needed. We shall rather insist on what is making ALARO’s spirit and structure, maintained and enhanced (respectively) at each stage of its continuously controlled evolution.

In short, ALARO can be characterised by: i) concern for a multi-scale operational behaviour (especially in view of grey-zone issues); ii) reliance on dimensioning algorithmic choices; iii) attempt at anticipating future core evolutions in a few selected aspects. We shall now review each of these three main characteristics and give some explanatory steps towards more concrete realisations. For the sake of simplicity, only atmospheric vertical column aspects will be addressed here, even if there is equal concern in implementation plans for 3D turbulence and for “memory via dynamics”.

Concerning ALARO practical results, there exists (yet) no NWP-related transversal article. But there is an interesting equivalent for the climate-type downscaling of quantitative extreme precipitation forecasts (De Troch et al. 2013). The version used in that paper is rather close to the ALARO-0 baseline.

1 A multi-scale system

The basic idea behind the multi-scale orientation of ALARO R&D efforts is to go directly for a grey-zone challenge. It means not to try and artificially blend developments coming from several scale-analyses, but rather to think in terms of “who can the most also can the least”. The tactics to successfully confront a difficulty happening mainly at a specific range of resolutions ought to deliver parameterisation schemes with a high potential of adaptation to other conditions. This happens then in principle without risk of self-contradiction. One key illustration of this orientation is the clear preference for a *convection permitting* strategy instead of a *convection resolving* one. We shall now see three concretisations of such a type of approach.

1.1 Full cloud-radiation interaction

As horizontal resolutions increase, more and more attention is logically paid to microphysics of clouds, with a clear prognostic orientation. It is therefore surprising that,

despite claims that cloud-radiation interaction is of fundamental importance, most radiation schemes for NWP applications consider this interaction with a degraded time- or space-scale (or both). This happens because such radiative transfer schemes privilege the CPU-costly absolute accuracy of optical effects' spectral handling. By doing so, they become so expensive for each realisation that they must be called only selectively. Much of the detailed information about model-clouds optical characteristics is then lost at higher scales and/or frequencies. What is tried in ALARO, via the development of ACRANEB2 (just concluded for its first version), is to parameterise as exactly as possible spectral aspects within a broadband bulk approach. This is done in order to also call with intermittency the gaseous absorption aspects of this parameterisation. But radiative fluxes corresponding to the actual situation in terms of surface, aerosols and clouds are computed in each grid-point and at each time-step. This selective intermittency approach may even be made more sophisticated by a split of its gaseous part between two levels, for best reaching the required accuracy (see below). For details about ACRANEB2 main characteristics, see Appendix A.

1.2 Merging local and self-organised aspects of moist turbulence

Time will come, and perhaps sooner as anticipated, when models will have to deal with grey zone aspects of shallow-convection. For the grey-zone of deep convection, what currently happens is that schemes traditionally relying on a separation of processes (stratiform vs. convective) encounter many serious problems. It can be argued that the same might happen in the future for schemes supposedly matching the scale separation between randomly acting and self-organised turbulent motions. In the ALARO framework, it appeared safer to bet on the well-established analogy between skewness-aware higher-order concretisations of Reynolds Stress Modelling (RSM) and the theoretical basis of mass-flux formulations for plumes. Of course, for keeping within NWP constraints, this requires carefully reducing the complexity of so-called Third Order Moment RSM schemes to a necessary minimum and nothing more. But there are (often neglected) proposals for this in the literature, e.g. Canuto et al. (2007) and Zilitinkevich et al. (2013). Furthermore handling of sub-grid condensation/evaporation aspects must cleanly interact with the resulting reduced-complexity synthetic framework. Here the idea is to combine a further reliance on the analogy with mass-flux computations and a return to basic Laws of thermodynamics. All this creates a rather new system, with quite a lot of side-options, but a strong backbone of key hypotheses, named TOUCANS (Third Order moments Unified Condensation Accounting and N-dependent Solver (for turbulence and diffusion)). For more details about this on-going but nearly completed development effort, see Appendix B.

1.3 Avoiding the resolved vs. parameterised deadlock for deep convection

It can be safely said that the heart of the ALARO R&D effort is the so-called 3MT (Modular Multi-scale Microphysics-Transport) scheme for handling most aspects of the atmospheric water cycle (apart from turbulent transport and cloud-radiation interactions, see above). 3MT touches so many aspects of the feed-backs that determine the model-atmosphere's behaviour that it is difficult to characterise it synthetically. One may however try two ways to make 3MT's spirit clearer. One might first say that 3MT is a way to do as if deep convection would be resolved but without needing to go to the hectometric scales where this is systematically true. As a second (analytical) interpretation, 3MT can be

said to result from the conjunction of ideas that:

- i. a maximum of prognostic character is needed to relax usual large-scale-type hypotheses made in classical mass-flux schemes, when going to higher resolutions;
- ii. there is only one type of clouds from the microphysical point of view (and that the resolved vs. parameterised grey-zone dilemma thus only exists when people insist on having closed algorithms on each side);
- iii. that the key issue is therefore to imagine (like in radiation) a correct and sophisticated interaction between cloud geometry and basic physical processes (here: auto-conversion, collection, phase changes during precipitation, and sedimentation).

3MT's choices are thus initially targeted to the deep convective grey-zone scales (typically for horizontal mesh-sizes between $\sim 1\text{km}$ and $\sim 7\text{km}$). But asymptotic behaviours on each side are nearly fully consistent with “resolved microphysics \Leftrightarrow dynamics” on the one side and with “classical mass-flux schemes with an implicit stationary-clouds assumption” on the other side. For more details see Gerard et al. (2009) and/or Appendix C (the latter complementing the said paper by insisting on a comprehensive -and original- microphysical treatment of phenomenological convective clouds/precipitations).

2 Importance of algorithmic choices

The second characteristic of ALARO is that some particular attention paid to algorithmic at a so-called mid-level (i.e., neither for the detailed description of basic physical properties/phenomena, nor for the overall precise structure of the physical time-step) is the key for fulfilling the above-mentioned aims. Furthermore this idea is mostly concretised in trying to get the longest possible time-steps whatever the spatial resolution rather than artificially stabilising an explicit-type procedure first developed with only short time-steps in mind. We shall again concentrate on practical manifestations of this strategy, with four examples this time.

2.1 Moist thermodynamics for a clean and self-consistent phys-dyn interfacing

Ensured total moist specific enthalpy conservation is in principle the key to avoid both spurious sources/sinks and artificial compensations of errors in physics-dynamics interfacing. However careful analysis shows that this is not as straightforward as could be thought. One effectively needs:

- i. a self-consistent and well-applied corpus of simplifying hypotheses;
- ii. verification that the latter corresponds to conservation of moist specific entropy for reversible transformations;
- iii. a barycentric view of the differential motions of atmospheric species;
- iv. a strict application of the Green-Ostrogradsky theorem, on the basis of summation of fluxes (physical quantities) rather than of individual tendencies (arbitrarily defined entities) when combining the effects of various parameterisation schemes.

All this is ensured in ALARO through using the Catry et al. (2007) framework, with the work of Marquet (2011) as additional justification (they share exactly the same set of simplifying hypotheses). This is of course fully applicable to other parameterisation sets than the ALARO one.

2.2 Using the NER hierarchy for cheap broad-band gaseous transmissivities

The ACRANE2 development strongly relies on the Net Exchanged Rates (NER) method (Green 1967) and on the idea of its application via acceptance of differing levels of accuracy for NER terms of various weights in the atmospheric thermal radiative budget. This double concept, pioneered by Joseph and Bursztyn (1976), surprisingly did not get any offspring for nearly thirty years, but there is now a renewed interest for it (Eymet et al. 2004). Application of this method to ACRANE2 is in fact much compatible with the aim of getting precision without using a fine-grained spectral discretisation. It is also well adapted to a technical separation of gaseous and cloudy-type optical effects in a first level intermittency strategy caring for the best possible interaction between both. In short:

- i. Cooling To Space (CTS) and Exchange With Surface (EWS) terms are computed as exactly as feasible;
- ii. Exchange between Adjacent Layers (EAL) terms are only slightly parameterised;
- iii. Exchange Between (non-adjacent) Layers (EBL) terms are diagnosed at each time-step from CTS, EWS and EAL characteristics. The relevant dependency is exactly assessed at quite long time intervals (there is thus a double intermittency strategy at work).

2.3 A simplified but fully consistent MY-Level-3 moist system for all stability conditions

The TOUCANS main target is to try and build a package for computation of moist turbulent fluxes (of momentum, heat, water vapour as well as cloud condensed water) as self-consistent as possible at Level 3 of the Mellor-Yamada (MY) classification. But this should happen with modularity in as many as possible issues, especially where competing theories are still being discussed [e.g. “No Ri(cr) MY” (Canuto et al. 2008), QNSE (Sukoriansky et al. 2005) and EFB (Zilitinkevich et al. 2008, 2013) for what touches energy conversion and anisotropy impacts]. Pillars of the TOUCANS discretisation choices are:

- i. turbulent energy sources and sinks always computed from flux time gradient considerations and as consistently as possible with the turbulent length scale’s specification;
- ii. prognostic treatment of both Turbulent Kinetic Energy (TKE) and Total Turbulent Energy (TTE);
- iii. stability dependency functions computed in relation to a single parameter, by using the solution of a Level 2 MY-type system as “slow-manifold” for the above prognostic aspects; this pushes one step further the by-and-large underexploited ideas of Redelsperger et al. (2001);
- iv. solving the same equations (via a targeted compact model of stability dependencies) from the most unstable up to the most stable situations; using Third Order Moments (TOMs) is essential in the first case as well as ensuring absence of any critical Richardson number in the second case;
- v. introduction of moist aspects via “specific moist entropic” considerations both (but separately) for buoyancy flux considerations and for determination of the neutral behaviour of anisotropy-linked stability dependency functions.

All these issues required specific algorithmic developments. Those were all realised in the above-mentioned spirit of allowing emulation of various modern options when returning to the physics of parameterised phenomena.

2.4 Separated deep convective microphysics & transport and summed resolved & parameterised condensation/evaporation rates

Concerning 3MT, making the central Microphysics-Transport (M-T) choice means that, contrary to what happens in classical mass-flux-type convective parameterisations, the hypothesis of stationary behaviour of the cloud ascent (both in size and in characteristics) is abandoned (Piriou et al. 2007). Drawing all consequences of this decision leads to:

- i. a prognostic closure and a partly-prognostic entrainment rates' specification (as a strong consequence, detrainment rates do not need any more to be parameterised); the starting point is here Gerard and Geleyn (2005), inspired by Chen and Bougeault (1992); but recent (unpublished) developments led to a CAPE-type mitigation of the moisture convergence closure and to a dependency of the buoyancy-sorting-type entrainment algorithm on past history of evaporation rates, a bit alike in the Mapes and Neale (2011) proposal;
- ii. an open-ended conclusion of the purely convective computations (updraft and downdraft) where only sub-grid transport fluxes and (respectively) condensation and evaporation rates are provided;
- iii. a need to care with particular attention to the interplay with non-convective condensation-evaporation processes.

The interplay with parameterisations of shallow-convection (via TOUCANS) and of cloud-radiation interactions (via ACRANE2) of course also needs attention.

3 Targeted novelties

As seen at the beginning of this note, ALARO tries to incorporate new (or revived) findings when this does not endanger application of the two basic concepts detailed in Sections 1 and 2 above. We shall here briefly mention five such items.

3.1 Specific moist entropic view of shallow convection

As already mentioned, the recent work of Marquet (2011) about a definition of specific moist air entropy θ_s conserved in both advective and mixing processes is used as an additional justification for choosing the Catry et al. (2007) proposal in interfacing physics and dynamics. But part of TOUCANS developments is also considering the additional result that nature tends to mix well θ_s in moist turbulent processes. The consequence of this observed fact is that the total water (q_t) flux should become the dominant term within energy conversion (or buoyancy term), when moist turbulent equations are rewritten in terms of $\theta_s \approx \theta_l e^{\Lambda q_t}$ and q_t (Marquet and Geleyn 2013). The moist equivalent potential temperature θ_l (or rather its static-energy-type equivalent) and q_t are still however the diffused quantities, also used for energy-related computations.

3.2 Revising one emissivity method hypothesis for better NER use

During the development of ACRANE2, the main hurdle preventing a satisfying “fit and use” of broadband thermal gaseous transmission functions was not the difficulty to parameterise saturation beyond classical band model solutions (e.g. Malkmus’ one in our case). It was in fact the up to now apparently undisputed opinion that applying the Curtis-Godson approximation may also encompass inside vertical integration operators variations of the Planck function’s relative weighting. A novel method was then developed to overcome this obstacle at reasonable cost, via a Taylor-first-order commutation between the bulk spectral integration and the weighting function’s derivation with respect to temperature.

3.3 Making an implicit use of the PDF information about entropy and moisture

The need of precisely accounting for cloud geometry in radiation and microphysics calculations was already mentioned. Concerning the various roles of cloudiness, the other main idea in ALARO is to resolutely go towards a fully implicit handling of Probability Distribution Functions (PDFs) of sub-grid variances and co-variances for humidity and heat. This should happen via (at least) three choices:

- i. reliance on the observed de-correlation between θ_s and q_t (see above);
- ii. use of the Xu and Randall (1996) formalism for the thermodynamic adjustment process, with some nice analytical properties being then used to parameterise the interplay between resolved and convective condensation-evaporation rates;
- iii. adaptation of the mass-flux concept to shallow convection, not in the classical way of an addition to local turbulent effects, but rather via the (initially mostly unnoticed) proposal of Lewellen and Lewellen (2004), combined with the already mentioned specific moist entropic considerations.

3.4 Going from “advective” to “statistic” for precipitations’ sedimentation

When ACRANE2 and TOUCANS will be fully stabilised, the most likely weakest point of ALARO will be its set of parameterisation steps for microphysical basic processes (at a rather middle sophistication level, in the line of Lopez (2002), see Appendix C). But it is at the same time the easiest part where to introduce more sophisticated variants, i.e. for auto-conversion, collection or phase changes of falling species. This happens thanks to a modularity-oriented combination of the above-mentioned geometrical considerations and of an interpretation of precipitating species’ sedimentation not as an advective process but as a statistical propagation one (Geleyn et al. 2008). Not only does the latter proposal provide a cheaper analytical solution, but it also makes the code interaction with other microphysical processes completely transparent to any of their particular details.

3.5 Cellular Automata as paradigm for the hidden sides of sub-grid convection

As explained in Bengtsson et al. (2013) the 3MT prognostic closure is particularly well suited for interacting with a Cellular Automaton (CA) tailored for simulating stochasticity, sub-grid memory and laterality of the convective behaviour at the finest possible

scales. Integrating this R&D effort into ALARO-1 is the next priority after moving to ACRANE2, TOUCANS and replacement of the 3MT saturated downdrafts algorithm by the handling of an unsaturated downdrafts more physical variant.

4 About consistency and unification of cloud-cover

Appendices A, B and C were already mentioned. In order to further synthesise innovative and rationalising aspects of ALARO, a rather technical Appendix D (previously prepared for planning purposes) presents a roadmap for a controlled evolution towards some unification of the cloud-cover concept within ALARO-1. After careful analysis concerning this important issue, it was decided not to aim at a single computation of cloudiness, like for instance in Tompkins (2002). What is the alternative ALARO approach is to build a “roundelay” of bilateral correspondences and/or combinations for all cases where two parameterisations interact at the level of the cloud-cover definition. For a practical concretisation of this idea, see in particular the Summary at the end of Appendix D. Upgrades with respect to ALARO-0+ACRANE2+TOUCANS needed for getting a first version of this unification (all identified in the Appendix text) are in fact relatively small. So testing of this transversal change, obviously touching many feed-back loops and hence unpredictable in its practical consequences, may start mid-2014. A diagram of the foreseen “physical time-step organisation” is shown after Appendix D.

References

- Bengtsson, L., M. Steinheimer, P. Bechtold, and J.-F. Geleyn, 2013: A stochastic parameterisation for deep convection using cellular automata. *Quart. J. Roy. Meteor. Soc.*, **139**, 1533–1543.
- Canuto, V., Y. Cheng, and A. Howard, 2007: Non-local ocean mixing model and a new plume model for deep convection. *Ocean Modelling*, **16**, 28–46.
- Canuto, V., Y. Cheng, A. Howard, and I. Esau, 2008: Stably stratified flows: A model with No Ri(cr). *J. Atmos. Sci.*, **65**, 2437–2447.
- Catry, B., J.-F. Geleyn, M. Tudor, P. Bénard, and A. Trojáková, 2007: Flux-conservative thermodynamic equations in a mass-weighted framework. *Tellus*, **95A**, 71–79.
- Chen, D. H. and P. Bougeault, 1992: A simple prognostic closure assumption to deep convective parameterization. *Acta Meteorologica Sinica*, **7**, 1–18.
- De Troch, R., R. Hamdi, H. V. de Vyver, J.-F. Geleyn, and P. Termonia, 2013: Multi-scale performance of the ALARO-0 model for simulating extreme summer precipitation climatology in Belgium. *J. Climate*, **26**, 8895–8915.
- Eymet, V., J.-L. Dufresne, P. Ricchiazzi, R. Fournier, and S. Blanco, 2004: Long-wave radiative analysis of cloudy scattering atmospheres using a net exchange formulation. *Atmos. Res.*, **72**, 239–261.
- Geleyn, J.-F., B. Catry, Y. Bouteloup, and R. Brožková, 2008: A statistical approach for sedimentation inside a microphysical precipitation scheme. *Tellus*, **60A**, 649–662.
- Gerard, L. and J.-F. Geleyn, 2005: Evolution of a subgrid deep convection parameterization in a limited-area model with increasing resolution. *Quart. J. Roy. Meteor. Soc.*, **131**, 2293–2312.

- Gerard, L., J.-M. Piriou, R. Brožková, J.-F. Geleyn, and D. Banciu, 2009: Cloud and precipitation parameterization in a meso-gamma-scale operational weather prediction model. *Mon. Wea. Rev.*, **137**, 3960–3977.
- Green, J., 1967: Division of radiative streams into internal transfer and cooling to space. *Quart. J. Roy. Meteor. Soc.*, **93**, 371–372.
- Joseph, J. and R. Bursztyn, 1976: A radiative cooling model in the thermal infrared for application to models of the general circulation. *Journal of Applied Meteorology*, **15**, 319–325.
- Lewellen, D. C. and W. S. Lewellen, 2004: Buoyancy flux modeling for cloudy boundary layers. *J. Atmos. Sci.*, **64**, 1147–1160.
- Lopez, P., 2002: Implementation and validation of a new prognostic large-scale cloud and precipitation scheme for climate and data assimilation purposes. *Quart. J. Roy. Meteor. Soc.*, **128**, 229–258.
- Mapes, B. and R. Neale, 2011: Parameterizing convection organisation to escape the entrainment dilemma. *J. Adv. Model. Earth Sys.*, **3**, Art. M06 004/(20 pp).
- Marquet, P., 2011: Definition of a moist entropy potential temperature: application to FIRE-I data flights. *Quart. J. Roy. Meteor. Soc.*, **137** (656), 768–791.
- Marquet, P. and J.-F. Geleyn, 2013: On a general definition of the squared Brunt–Väisälä frequency associated with the specific moist entropy potential temperature. *Quart. J. Roy. Meteor. Soc.*, **139** (670), 85–100.
- Piriou, J.-M., J.-L. Redelsperger, J.-F. Geleyn, J.-P. Lafore, and F. Guichard, 2007: An approach for convective parameterization with memory, in separating microphysics and transport in grid-scale equations. *J. Atmos. Sci.*, **64**, 4127–4139.
- Redelsperger, J., F. Mahé, and P. Carlotti, 2001: A simple and general subgrid model suitable both for surface layer and free-stream turbulence. *Bound.-Layer Meteor.*, **101**, 375–408.
- Sukoriansky, S., B. Galperin, and I. Staroselsky, 2005: A quasi-normal scale elimination model of turbulent flows with stable stratification. *Physics of fluids*, **17**, 085107–1–28.
- Tompkins, A., 2002: A prognostic parameterization for the subgrid-scale variability of water vapor and clouds in large-scale models and its use to diagnose cloud cover. *J. Atmos. Sci.*, **59**, 1917–1942.
- Xu, K. M. and D. Randall, 1996: A semi-empirical cloudiness parameterization for use in climate models. *J. Atmos. Sci.*, **53**, 3084–3102.
- Zilitinkevich, S., T. Elperin, N. Kleeorin, I. Rogachevskii, and I. Esau, 2013: A hierarchy of energy- and flux-budget (EFB) turbulence closure models for stably-stratified geophysical flows. *Bound.-Layer Meteor.*, **146**, 341–373.
- Zilitinkevich, S., T. Elperin, N. Kleeorin, I. Rogachevskii, I. Esau, T. Mauritsen, and M. W. Miles, 2008: Turbulence energetics in stably stratified geophysical flows: Strong and weak mixing regimes. *Quart. J. Roy. Meteor. Soc.*, **134**, 793–799.

Appendix A: Overview of ACRANEB2 radiative transfer scheme

J. Mašek

This appendix describes main novelties of ACRANEB2 radiative transfer scheme. First subsection lists starting assumptions and simplifying hypotheses used in original ACRANEB scheme. With only few minor exceptions, they are reused in ACRANEB2 scheme. Following subsections describe most important developments concerning gaseous transmissions, thermal exchanges, cloud optical properties and surface albedo. Final subsection compares CPU cost of ACRANEB, ACRANEB2 and RRTM/FMR radiation schemes, employing various intermittent strategies.

A.1 Main ACRANEB features

ACRANEB is an economical radiation transfer scheme, used in model ALADIN since 1990s. Its design is a compromise between cost and accuracy, having following key features:

- broadband approach with electromagnetic spectrum split into single shortwave (solar) and single longwave (thermal) interval
- assumption of random spectral overlaps between various radiatively active species, alias additivity of their optical depths
- atmospheric column consisting of plane-parallel homogeneous layers, each layer divided to clearsky and cloudy parts, with no lateral exchanges between them
- random or maximum-random cloud overlap assumption applied at layer interfaces to redistribute fluxes leaving cloudy and clearsky parts
- multiple scattering accounted for by delta-two stream approximation combined with adding method (chosen system assumes hemispherically constant intensities and delta-scaled phase function linear in cosine of scattering angle)
- absorbing gases H_2O , O_3 and CO_2+ (composite of CO_2 , N_2O , CO , CH_4 and O_2 , i.e. most important radiatively active gases with constant mixing ratios with respect to dry air)
- impact of scattering on gaseous absorption treated by method of idealized optical paths
- saturation of gaseous absorption based on Malkmus band model with empirical broadband correction
- non-homogeneous gaseous optical paths treated by Curtis-Godson approximation
- cloud optical properties updated at every timestep (important for full radiative feedback of model cloudiness)
- cloud optical saturation based on concept of effective cloud optical depth
- aerosols and surface treated as grey bodies
- longwave computations based on NER (Net Exchanged Rate) formalism

- exchanges between layers evaluated using bracketing technique with statistically fitted weights, ensuring a cost linear in number of levels

In spring 2011, work on improved gaseous transmissions started, since they were felt as the weakest part of the ACRANE scheme. It revealed several fundamental problems and initiated changes also in NER part and in parameterization of cloud optical properties. All these developments became part of the new scheme named ACRANE2.

A.2 Gaseous transmissions

Original ACRANE gaseous transmissions were based on AFGL 1980 data tape. This is a quite outdated source of spectroscopic data, with several known deficiencies (some weaker lines are missing, temperature exponent for line half widths uses classical value $\frac{1}{2}$, data for ozone absorption are incomplete). Moreover, transmission fits for CO₂+ composite were done using IPCC 1990 concentrations and H₂O e-type continuum was treated in semi-empirical way. ACRANE2 gaseous transmissions are fitted against reference based on the more recent HITRAN 2008 line parameters, complemented by Serdyuchenko et al. (2013) dataset for shortwave ozone continuum absorption. CO₂+ composite was updated to WDCGG 2010 concentrations and CO was excluded due to its negligible radiative impact in both shortwave and longwave parts of spectrum. Data for longwave H₂O e-type continuum were imported from model MT_CKD version 2.5.2, since it was discovered that the old semi-empirical treatment led to exaggerated temperature dependency.

In ACRANE, dependency of broadband gaseous optical depths on absorber amount u was fitted using Malkmus formula

$$\delta_{\text{malkmus}} = \frac{a}{2b}(\sqrt{1 + 4bu} - 1), \quad (\text{A1})$$

followed by 10-parametric Pade correction. In ACRANE2, fitted temperature dependency of broadband Malkmus coefficients a and b was changed from power law to cheaper hyperbolic shape:

$$a(T) = a_0 \cdot \frac{1 + a_1 T}{1 + a_2 T} \quad b(p, T) = \frac{b_0}{p} \cdot \frac{1 + b_1 T}{1 + b_2 T} \quad (\text{A2})$$

$$a_0, b_0 > 0 \quad a_1, a_2, b_1, b_2 \geq 0$$

Aim of the a posteriori Pade correction was to account for the fact that averaging of narrowband optical depths given by Malkmus formulas does not result in Malkmus formula.¹ Manifestation of this fact is so-called secondary saturation, felt as slower than \sqrt{u} growth of broadband optical depth δ for big absorber amounts u . However, original Pade correction was unable to change $\log(\delta)$ - $\log(u)$ slope in big u limit. It was therefore replaced by simpler 2-parametric rescaling of broadband optical depth δ_{malkmus} , with pressure and temperature independent fitting parameters α and δ_0 :

$$\delta = \frac{\delta_0}{\alpha} \left[\left(1 + \frac{\delta_{\text{malkmus}}}{\delta_0} \right)^\alpha - 1 \right] \quad (\text{A3})$$

$$0 < \alpha < 1 \quad \delta_0 > 0$$

For $\delta_{\text{malkmus}} \ll \delta_0$ above formula reduces to identity, while for $\delta_{\text{malkmus}} \gg \delta_0$ it gives growth proportional to $(\delta_{\text{malkmus}})^\alpha$, resulting in $\log(\delta)$ - $\log(u)$ slope approaching $\frac{\alpha}{2}$ for $u \rightarrow \infty$. It proved to be fully sufficient for describing secondary saturation.

¹Spectral averaging must of course be applied on transmissions $\tau = \exp(-\delta)$, not directly on optical depths δ .

Tests in isothermal atmosphere proved superiority of ACRANEB2 broadband gaseous transmissions over ACRANEB ones. Still, to get heating rates within 0.1 K/day from narrowband reference, 8 fitting parameters (i.e. $a_0, a_1, a_2, b_0, b_1, b_2, \alpha$ and δ_0) per gas and spectral band turned out to be insufficient. Pressure and temperature dependent secondary corrective fits had to be introduced, bringing 25 additional fitting parameters for each gas and spectral band. Their application to non-homogeneous optical paths requires use of explicitly averaged pressure and temperature, possibly inconsistent with implicit averaging present in Curtis-Godson approximation. Anyway, tests showed that this inconsistency does not lead to any serious problem and that secondary corrective fits are clearly beneficial.

Moving to non-isothermal atmosphere revealed a fundamental problem with longwave gaseous transmissions. They were fitted against broadband reference computed by spectral averaging of narrowband transmissions, using Planck weights $\pi B_\nu(T)/(\sigma T^4)$ with local temperature T (where $B_\nu(T)$ is Planck function and σ is Stefan-Boltzmann constant). However, correct weights should use temperature of emitting body T_e , which can be very different from local temperature T . It means that homogeneous longwave gaseous transmissions should not be just function of absorber amount u , local pressure p and local temperature T , but they should depend on temperature of emitting body T_e as well. Figure A1 demonstrates both accuracy of ACRANEB2 fits in isothermal case (left panel) and deterioration caused by $T_e = T$ assumption in non-isothermal case, where heating rate error reaches ~ 0.4 K/day (right panel). Reference heating rates were obtained by emissivity type computation which used spectrally averaged narrowband transmissions with temperature T_e in Planck weights. There was thus no broadband fitting involved in the reference computations.

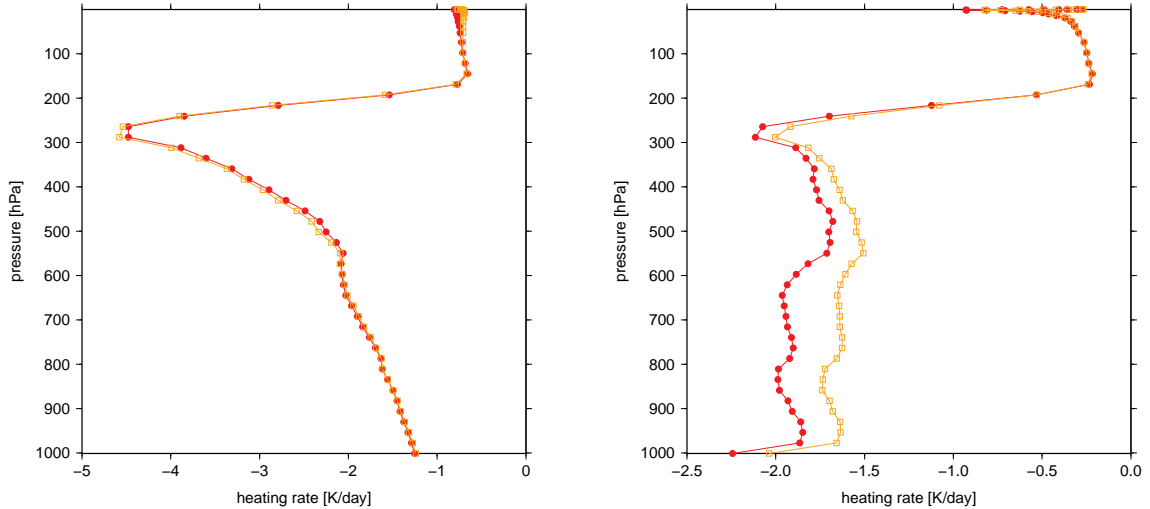


Figure A1: H_2O longwave heating rates without e-type continuum for isothermal (left) and non-isothermal (right) clear-sky atmosphere: red – reference obtained by emissivity type computation; yellow – broadband computation with $T_e = T$ assumption.

To cure the problem, ACRANEB2 uses first order T_e correction, obtained by linearization of Planck weights with respect to temperature around value $T_0 = 255.8$ K. It is then sufficient to have two sets of longwave transmissions – first computed with $\pi B_\nu(T_0)/(\sigma T_0^4)$ weights, second with $\pi dB_\nu/dT(T_0)/(4\sigma T_0^3)$ weights. Resulting T_e corrected transmission

then reads:

$$\tau_{B(T_e)} = \tau_{B(T_0)} + 4 \left(\frac{T_e}{T_0} - 1 \right) [\tau_{dB/dT(T_0)} - \tau_{B(T_0)}] \quad (\text{A4})$$

Tests done in emissivity type computation proved that for the meteorological range of temperatures, the above linearization of Planck weights with respect to T_e is fully sufficient.

Last problem with gaseous transmissions was encountered when several absorbing gases are present. In ACRANEb it was assumed that broadband optical depths of various gases are additive, which is equivalent to their random spectral overlaps. However, it was found that in longwave part of spectrum this assumption is not realistic and effect of non-random spectral overlaps must be parameterized. There was an earlier attempt to do that in ACRANEb, based on dominant role of pair gaseous overlaps. Even if it never entered operations, it was used as starting point for the new overlap parameterization working in absorptivity space, where it was possible to reduce 4-dimensional fitting problem to 1-dimensional. The fitting dependency for broadband pair overlap has the shape:

$$a - a_{\text{rand}} = f(a_1, a_2) A (1 - a_{\text{rand}})^B a_{\text{rand}}^C (1 - D a_{\text{rand}}), \quad (\text{A5})$$

$$a_{\text{rand}} = a_1 + a_2 - a_1 a_2 \quad f(a_1, a_2) = \frac{2a_1 a_2}{\epsilon + a_1^2 + a_2^2} \quad \epsilon = 10^{-20}$$

Here $a \equiv 1 - \tau$ is absorptivity of the mixture, a_{rand} is absorptivity of the mixture assuming random spectral overlaps, $f(a_1, a_2)$ is modulation factor and a_1, a_2 are absorptivities of individual gases. There are 4 fitting parameters A, B, C and D .

The modulation factor $f(a_1, a_2)$ is less or equal to one and it accounts for the fact that overlap effect becomes less important when broadband absorption of the two gases is very different in magnitude. It contains a small quantity ϵ to prevent division by zero when $a_1 = a_2 = 0$.

Figure A2 shows typical performance of longwave overlap fit (A5). Figure A3 demonstrates disastrous impact of random gaseous overlaps in longwave part of spectrum (yellow curve versus red). It also shows that fitting error of non-random pair overlaps combined with error coming from neglected ($\text{H}_2\text{O}, \text{O}_3, \text{CO}_2+$) triple overlap is acceptable (green curve versus red). In shortwave part of the spectrum, impact of non-random gaseous overlaps is weak, so their parameterization was switched off for efficiency reasons.

A.3 NER scheme and bracketing

Main idea of NER technique is to split longwave exchanges into primary (cooling to space CTS, exchange with surface EWS and exchange between adjacent layers EAL) and secondary (exchange between non-adjacent layers EBL). Dominant primary exchanges are computed as exactly as possible, with cost being linear in number of levels. Secondary exchanges are approximated, since the cost of their exact computation would be quadratic in number of levels and since they represent a smaller contribution to the total effect. Estimation of EBL flux in ACRANEb is done via so-called bracketing technique. It employs minimum and maximum layer optical depths (obtained from CTS, EWS and EAL computations) to estimate minimum and maximum EBL fluxes. True EBL flux is then statistically fitted as

$$\text{EBL} = (1 - \alpha) \text{EBL}_{\text{min}} + \alpha \text{EBL}_{\text{max}}, \quad (\text{A6})$$

where $0 \leq \alpha \leq 1$ is bracketing weight. Stratification of big amount of data obtained from global model runs revealed that weight α depends both on σ -coordinate (distant exchanges are generally more important in high atmosphere) and stability (temperature inversions

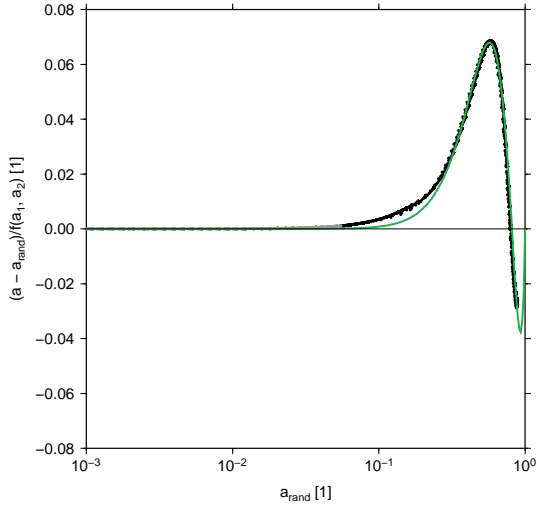


Figure A2: Longwave overlap fit for (H_2O , CO_2+) gaseous pair. Data points for modulation factors bigger/smaller than $10^{-\frac{1}{2}}$ are black/grey, fitted dependency is green.

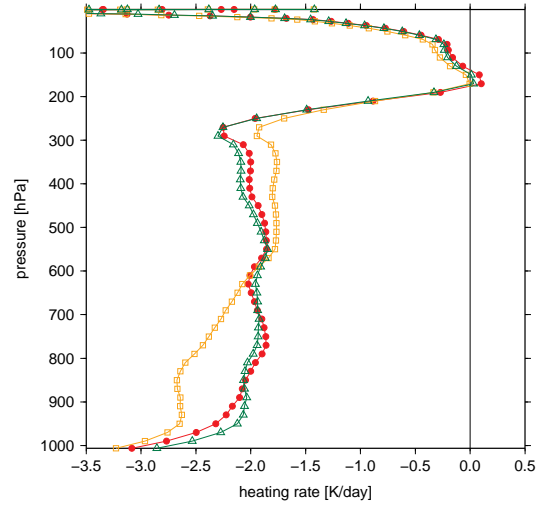


Figure A3: Longwave heating rates for mid-latitude summer case containing H_2O , O_3 and CO_2+ : red – narrowband reference with explicit treatment of gaseous overlaps; yellow – ACRANEB2 assuming random gaseous overlaps; green – ACRANEB2 with parameterized non-random pair gaseous overlaps.

enhance local exchanges). ACRANEB scheme used 7-parametric fit of α with respect to σ and stability, still the spread of data points was too big, resulting in limited accuracy of statistical fit.

ACRANEB2 uses different approach. It does not fit bracketing weight α , but expresses true EBL flux as

$$\text{EBL} = A(\sigma)\text{EBL}_{\min} + B(\sigma)\text{EBL}_{\max}, \quad (\text{A7})$$

where A and B are second order polynomials in σ and they are not constrained to sum up to one. Figure 4 demonstrates that formula (A7) leads to a more accurate statistical fit than (A6). It can be inverted back to a bracketing weight α , which is however no longer constrained to interval $[0, 1]$.

Common disadvantage of statistical fits is their dependency on vertical resolution. Moreover, inclusion of cloudiness in ACRANEB2 currently disables exact computation of adjacent exchanges, crucial for accuracy of statistical fit (A7). To circumvent both problems, an alternative approach was implemented – exact computation of true EBL flux done at every n -th timestep, converted to bracketing weight α and stored for usage in intermediate timesteps. This strategy turned out to be successful thanks to the fact that time evolution of bracketing weight α happens on scales of hours, not faster.

A.4 Cloud optical properties

ACRANEB cloud optical properties were fitted against Stephens (1978) liquid clouds and Rockel et al. (1991) ice clouds. Cloud absorption and scattering coefficients are functions of liquid/ice water content and they are reduced by so-called saturation factors depending on effective cloud optical depth. It turned out that despite parameterization of broadband cloud optical saturation, ACRANEB ice clouds are too opaque. Therefore,

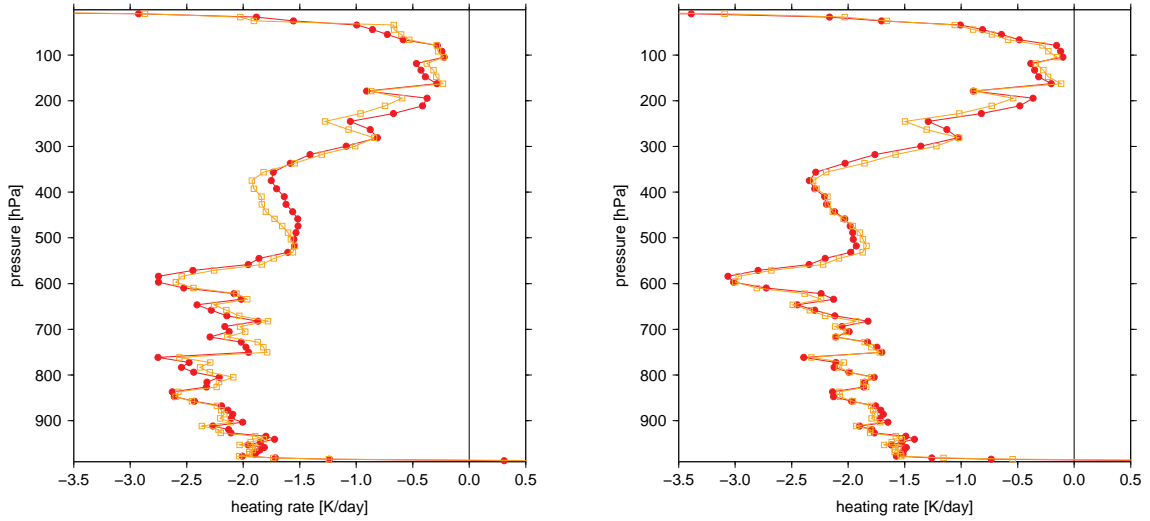


Figure A4: Accuracy of statistical fit in ACRANEB (left) and ACRANEB2 (right), demonstrated by longwave clearsky heating rates: red – exactly computed EBL; yellow – statistically fitted EBL.

in ACRANEB2 ice clouds were refitted using more recent Edwards et al. (2007) data. Broadband cloud optical saturation was unified with secondary saturation of gases given by a formula analogous to (A3). It is now active only for shortwave cloud absorption, since for scattering and in longwave part of spectrum cloud saturation starts to be significant only for optical depths ~ 10 or higher, i.e. when the corresponding transmission is practically zero.

A.5 Surface albedo

ACRANEB scheme uses Geleyn's formula for dependency of direct albedo α on cosine of solar zenithal angle μ_0 :

$$\alpha(\mu_0) = \frac{1 + \frac{\mu_0}{2} \left(\frac{1}{\bar{\alpha}} - 1 \right)}{\left[1 + \mu_0 \left(\frac{1}{\bar{\alpha}} - 1 \right) \right]^2} \quad (\text{A8})$$

Quantity $\bar{\alpha}$ is diffuse albedo and it is given by angular average

$$\bar{\alpha} = \frac{\int_0^1 \alpha(\mu_0) I(\mu_0) \mu_0 d\mu_0}{\int_0^1 I(\mu_0) \mu_0 d\mu_0} = 2 \int_0^1 \alpha(\mu_0) \mu_0 d\mu_0, \quad (\text{A9})$$

assuming hemispherically constant intensity of diffuse radiation $I(\mu_0)$, consistently with employed δ -two stream hypothesis.

Geleyn's formula (A8) realistically describes water surface (total reflection for sun on the horizon), but in ACRANEB scheme it was used above land as well. In order to have tunable angular dependency, proportion of Lambertian surface $0 \leq \lambda \leq 1$ was introduced in ACRANEB2, generalizing formula (A8) into the form

$$\alpha'(\mu_0) = (1 - \lambda)\alpha(\mu_0) + \lambda\bar{\alpha}, \quad (\text{A10})$$

where $\alpha'(\mu_0)$ and $\bar{\alpha}$ still respect angular constraint (A9). Lambertian proportion λ is given via namelist and has separate value for water and solid surfaces.

A.6 CPU cost

In order to have ACRANE2 scheme as efficient as possible, two level intermittency was implemented in longwave NER computations. Cloud optical properties are updated at every timestep, while gaseous transmissions and bracketing weights are updated only from time to time and stored for usage in subsequent timesteps. Numerical experiments have proven that it is fully sufficient to update gaseous transmissions every hour and bracketing weights every three hours. No intermittency was implemented in shortwave computations so far, since due to absence of exchanges they are much cheaper than longwave computations.

Efficiency of various radiation schemes and intermittent strategies is given in table below. Reference is 24 hour integration on operational CHMI domain ($\Delta x = 4.7$ km, 87 levels, $\Delta t = 180$ s), using ACRANE2 radiation scheme without any intermittency and with old statistical fit. Relative CPU cost was determined by dividing user time of given model run by user time of reference run, thus it can vary up to few percent due to actual machine load:

radiative scheme	update frequency			relative CPU cost
	clouds	gases	bracketing weights	
RRTM/FMR	3 min	3 min	–	2.40
RRTM/FMR	1 h	1 h	–	1.03
ACRANE2	3 min	3 min	3 min	1.49
ACRANE2	3 min	3 min	3 min, statistical fit	1.00 (reference)
ACRANE2	3 min	3 min	3 min	5.42
ACRANE2	3 min	1 h	3 h	1.07

It can be seen that without any intermittency, ACRANE2 integration is more than twice as expensive as RRTM/FMR integration and they are both not affordable compared to reference ACRANE2 integration. However, use of 1 h intermittency makes RRTM/FMR integration only 3% more expensive than ACRANE2 reference, while 1 h/3 h two level intermittency makes ACRANE2 integration 7% more expensive than the same reference. Main difference between the two configurations is update of cloud optical properties once per hour (RRTM/FMR), resp. 20 times per hour alias at every timestep (ACRANE2).

Figure A5 demonstrates that 1 h intermittency including clouds has quite some impact in RRTM/FMR, while 1 h/3 h two level intermittency excluding clouds is much less harmful in ACRANE2. And since RRTM/FMR scheme does not offer mixed solution with intermittency applied only to gaseous transmissions, few percent CPU increase of ACRANE2 scheme seems to be reasonable price for both improved gaseous transmissions and full feedback with clouds at the timestep scale.

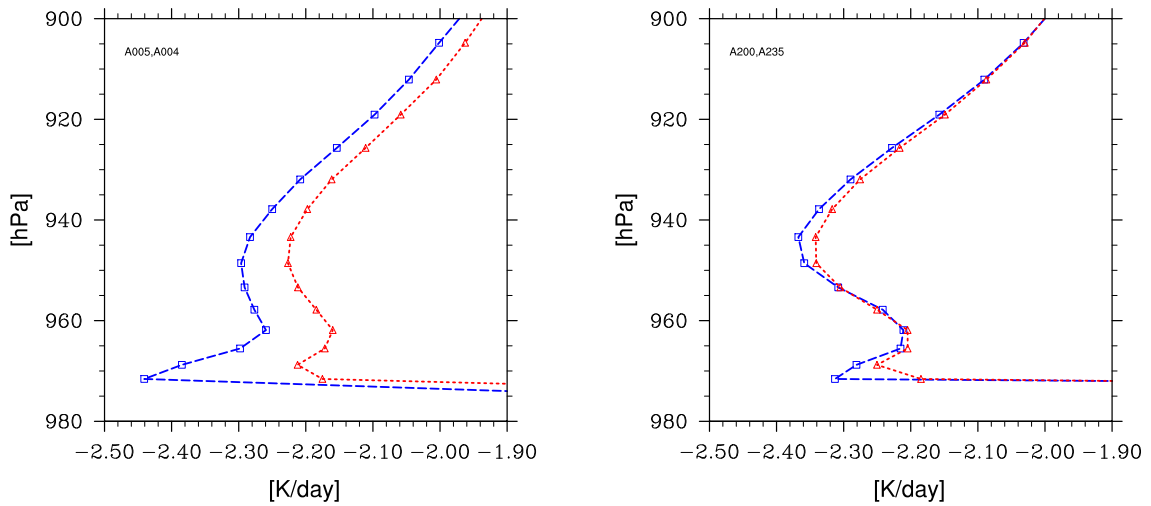


Figure A5: Impact of 1 h intermittency in RRTM/FMR (left) and 1 h/3 h two level intermittency in ACRANE2 (right), demonstrated on 12 hour domain averaged longwave heating rates: red – reference computation without any intermittency; blue – intermittent computation. Please keep in mind that RRTM/FMR intermittency applies also to clouds, while ACRANE2 intermittency does not.

Additional references

- Edwards, J., S. Havemann, J.-C. Thelen, and A. Baran, 2007: A new parameterization for the radiative properties of ice crystals: Comparison with existing schemes and impact in a GCM. *Atmos. Res.*, **83**, 19–35.
- Mlawer, E. J., V. H. Payne, J.-L. Moncet, J. S. Delamere, M. J. Alvarado, and D. D. Tobin, 2012: Development and recent evaluation of the MT-CKD model of continuum absorption. *Phil. Trans. Roy. Soc. A*, **370**, 1–37.
- Rockel, B., E. Raschke, and B. Weyres, 1991: A parameterization of broad band radiative transfer properties of water, ice and mixed clouds. *Beitr. Phys. Atmosph.*, **64**, 1–12.
- Rothman, L. S., et al., 2009: The HITRAN 2008 molecular spectroscopic database. *J. Quant. Spectrosc. Radiat. Transf.*, **110**, 533–572.
- Serdyuchenko, A., V. Gorshelev, M. Weber, W. Chehade, and J. P. Burrows, 2013: High spectral resolution ozone absorption cross-sections – Part 2: Temperature dependence. *Atmos. Meas. Tech. Discuss.*, **6**, 6613–6643.
- Stephens, G. L., 1978: Radiation profiles in extended water clouds. I: Theory. *J. Atmos. Sci.*, **35**, 2111–2122.

Appendix B: TOUCANS

I. Bařtak Duran

This Appendix summarises the main properties of TOUCANS (Third Order moments (TOMs) Unified Condensation Accounting and N-dependent Solver (for turbulence and diffusion)) turbulence parameterisation scheme.

An overview of the closure and discretisation method of TOUCANS is presented in the first Subsection. Details concerning influence of moisture in the scheme, choice of stability dependency functions, TOMs parameterisation and length scale computation then follow in the four subsequent Subsections. The last Subsection links all previous information pieces when describing the time-step organisation of TOUCANS.

B.1 Closure and discretisation

TOUCANS is a turbulence scheme with prognostic TKE and TTE. The evolution of both energies is influenced by advection, by their vertical turbulent diffusion, by dissipation terms ϵ and ϵ_{TTE} (see Zilitinkevich et al. 2013) and by contribution from source terms - shear (I) and buoyancy (II):

$$\frac{\partial e}{\partial t} = A_{\text{dvection}}(e) + \frac{\partial}{\partial z} \left(K_{\text{TKE}} \frac{\partial e}{\partial z} \right) + I + II - \epsilon, \quad (\text{B1})$$

$$\frac{\partial \text{TTE}}{\partial t} = A_{\text{dvection}}(\text{TTE}) + \frac{\partial}{\partial z} \left(K_{\text{TTE}} \frac{\partial \text{TTE}}{\partial z} \right) + I - \epsilon_{\text{TTE}}, \quad (\text{B2})$$

$$I = -\overline{u'w'} \frac{\partial \bar{u}}{\partial z} - \overline{v'w'} \frac{\partial \bar{v}}{\partial z}, \quad II = E_{s_{sL}} \overline{w's'_{sL}} + E_{q_t, s_{sL}} \overline{w'q'_t} \quad (\text{B3})$$

with $e = 0.5 (\overline{u'^2} + \overline{v'^2} + \overline{w'^2})$ the prognostic TKE, u, v and w wind components, K_{TKE} and K_{TTE} the TKE and TTE vertical exchange coefficients, $s_{sL} = c_{pd} \left(1 + \left[\frac{c_{pv}}{c_{pd}} - 1 \right] q_t \right) T + gz - (L_v q_l + L_s q_i)$ a diffused moist conservative variable, g gravitational acceleration, z height, c_{pd} and c_{pv} specific heat values for dry air and water vapour, L_v and L_s latent heats of vaporisation and sublimation, T temperature, q_t total specific water content, q_l and q_i specific contents for liquid and solid water, and $E_{q_t, s_{sL}}$ plus $E_{s_{sL}}$ the weights for computation of the buoyancy flux (see Subsection B.2).

The actual turbulent fluxes are computed from local gradients of diffused variables together with contributions from TOMs (based on Canuto et al. 2007) to heat and moisture fluxes (see Subsection B.4 for details):

$$\overline{w'u'} = -K_M \cdot \frac{\partial \bar{u}}{\partial z} \quad (\text{B4})$$

$$\overline{w'v'} = -K_M \cdot \frac{\partial \bar{v}}{\partial z} \quad (\text{B5})$$

$$\begin{aligned} \overline{w's'_{sL}} &= -K_H \cdot \frac{\partial \bar{s}_{sL}}{\partial z} \\ &- K_H \frac{O_\lambda T_H \tau}{C_3 e} \left[E_{s_{sL}} \frac{\partial \overline{w's'^2_{sL}}}{\partial z} - K^{(A_2, A_1)} \frac{\partial \bar{s}_{sL}}{\partial z} \frac{\partial \overline{w'^3}}{\partial z} + K^{(A_2, A_3)} \frac{1}{\tau} \frac{\partial \overline{w'^2 s'_{sL}}}{\partial z} \right] \end{aligned} \quad (\text{B6})$$

$$\begin{aligned} \overline{w'q'_t} &= -K_H \cdot \frac{\partial \bar{q}_t}{\partial z} \\ &- K_H \frac{O_\lambda T_H \tau}{C_3 e} \left[E_{q_t, s_{sL}} \frac{\partial \overline{w'q_t'^2}}{\partial z} - K^{(A_2, A_1)} \frac{\partial \bar{q}_t}{\partial z} \frac{\partial \overline{w'^3}}{\partial z} + K^{(A_2, A_3)} \frac{1}{\tau} \frac{\partial \overline{w'^2 q'_t}}{\partial z} \right] \end{aligned} \quad (\text{B7})$$

with K_M exchange coefficient for momentum, K_H rescaled (see below) exchange coefficient for heat and moisture, τ turbulence dissipation time scale for TKE, C_3 inverse Prandtl number at neutrality, O_λ free parameter, T_H a combined stability dependency function (see Subsection B.3), and $K^{(A_2, A_1)}$ and $K^{(A_2, A_3)}$ tuning constant terms. Note that the first terms in brackets on RHS in (B6) and (B7) have no tuning constant since they correspond directly to a TOM term in the prognostic Turbulent Potential Energy (TPE) equation (obtained from (B1) and (B2)).

The specific TOUCANS closure and discretisation method (simplified version of level 2.5/level 3 Mellor-Yamada-type model closures) uses TKE and TTE steady-state equilibrium values as targeted references. Hence a relaxation of TKE and TTE towards their equilibrium values - \tilde{e} and $\widetilde{\text{TTE}}$ - for the current time-step replaces in practice the source and dissipation terms in (B1) and (B2):

$$\frac{\partial e}{\partial t} = A_{\text{dvection}}(e) + \frac{\partial}{\partial z} \left(K_{\text{TKE}} \frac{\partial e}{\partial z} \right) + \frac{2}{\tau} (\tilde{e} - e), \quad (\text{B8})$$

$$\frac{\partial \text{TTE}}{\partial t} = A_{\text{dvection}}(\text{TTE}) + \frac{\partial}{\partial z} \left(K_{\text{TTE}} \frac{\partial \text{TTE}}{\partial z} \right) + \frac{2}{\tau_{\text{TTE}}} (\widetilde{\text{TTE}} - \text{TTE}), \quad (\text{B9})$$

$$\tilde{e} = \frac{\tau}{2} \left(-\overline{u'w'} \frac{\partial \bar{u}}{\partial z} - \overline{v'w'} \frac{\partial \bar{v}}{\partial z} + E_{s_{sL}} \overline{w's'_{sL}} + E_{q_{t,s_{sL}}} \overline{w'q'_t} \right), \quad (\text{B10})$$

$$\widetilde{\text{TTE}} = \frac{\tau_{\text{TTE}}}{2} \left(-\overline{u'w'} \frac{\partial \bar{u}}{\partial z} - \overline{v'w'} \frac{\partial \bar{v}}{\partial z} \right), \quad (\text{B11})$$

$$\tau = \frac{2L}{C_\epsilon F_\epsilon \sqrt{e}}, \quad \tau_{\text{TTE}} = \tau \frac{C_4(1+\Pi)}{C_4 + 2C_3\Pi}, \quad \Pi = \frac{\text{TTE}}{e} - 1 \quad (\text{B12})$$

with L turbulence length scale (see Subsection B.5), C_ϵ a free parameter, F_ϵ a combined stability dependency function, τ_{TTE} turbulence dissipation time scale for TTE and C_4 a closure coefficient.

In agreement with this, the three basic stability dependency functions χ_3 , ϕ_3 and ϕ_Q (see Subsection B.3 for details) in computation of exchange coefficients for momentum fluxes K_M and heat-moisture fluxes K_H are derived for equilibrium conditions:

$$K_M = \frac{\nu^4}{C_\epsilon} L \chi_3 (Ri_{f,s1}) \cdot \sqrt{e}, \quad (\text{B13})$$

$$K_H = C_3 \frac{\nu^4}{C_\epsilon} L \frac{2\phi_Q(Ri_{f,s1}) - [\phi_Q(Ri_{f,m}) - \phi_3(Ri_{f,m})]}{1 + \frac{\phi_Q(Ri_{f,m})}{\phi_3(Ri_{f,m})}} \sqrt{e}, \quad (\text{B14})$$

$$Ri_{f,m} = \frac{2C_3\Pi}{C_4 + 2C_3} \quad (\text{B15})$$

with ν a free parameter and $Ri_{f,m}$ and $Ri_{f,s1}$ stability parameters dimensioned like flux-Richardson numbers. While $Ri_{f,m}$ is linked to the conversion between TKE and TPE, $Ri_{f,s1}$ is related to the flux of conservative specific moist entropic potential temperature θ_{s1} (Marquet 2011):

$$Ri_{f,s1} = \frac{\frac{gM(S_{cc})}{\theta_{s1}} \overline{w'\theta'_{s1}}}{\overline{u'w'} \frac{\partial \bar{u}}{\partial z} + \overline{v'w'} \frac{\partial \bar{v}}{\partial z}} \quad (\text{B16})$$

with S_{cc} the Shallow Convection Cloudiness and $M(S_{cc})$ a function of it expressing the decrease of the resistance to vertical buoyant motions when S_{cc} increases (see Subsection B.2).

In TOUCANS $Ri_{f,s1}$ influences the anisotropy stability dependency functions - χ_3 and ϕ_Q - and $Ri_{f,m}$ is used in the conversion part of heat and moisture flux computation. Thus both conservation and conversion aspects are represented in the turbulent exchange coefficients.

B.2 Moist issue

The influence of moisture (via expansion and via latent heat release) is parameterised in TOUCANS through the use of the ‘moist’ buoyancy term II together with the corresponding ratio of turbulent energies Π (B12) as stability parameter. According to Marquet and Geleyn (2013) we can express moist buoyancy from fluxes of diffused variables and through the knowledge of S_{cc} :

$$II = E_{s_{sL}} \overline{w' s'_{sL}} + E_{q_t, s_{sL}} \overline{w' q'_t} \quad (\text{B17})$$

$$E_{s_{sL}} = \frac{g M(S_{cc})}{\bar{c}_p \bar{T}}, \quad (\text{B18})$$

$$E_{q_t, s_{sL}} = g M(S_{cc}) \left\{ \left(\frac{R_v - R_d}{R_d \cdot \bar{q}_d + R_v \cdot \bar{q}_v} - \frac{c_{pv} - c_{pd}}{\bar{c}_p} \right) + \widehat{Q}(S_{cc}) \left[\frac{L_{vs}(\bar{T})(R_d \cdot \bar{q}_d + R_v \cdot \bar{q}_v)}{\bar{c}_p \bar{T} R_v} - 1 \right] \left[\frac{R_v - R_d}{R_d \cdot \bar{q}_d + R_v \cdot \bar{q}_v} + \frac{1}{(1 - q_t)(1 + D_C)} \right] \right\} \quad (\text{B19})$$

$$M(S_{cc}) = \frac{1 + D_C}{1 + D_C F(S_{cc})} \quad (\text{B20})$$

$$F(S_{cc}) = 1 + S_{cc} \left[\frac{L_{vs}(\bar{T})(R_d \cdot \bar{q}_d + R_v \cdot \bar{q}_v)}{\bar{c}_p \bar{T} R_v} - 1 \right] \quad (\text{B21})$$

$$D_C = \frac{L_{vs}(\bar{T}) r_s^{li}}{R_d \bar{T}} = \frac{\bar{T}}{\bar{p} - e_{sat}(\bar{T})} \frac{\partial e_{sat}(\bar{T})}{\partial \bar{T}} \quad (\text{B22})$$

with R_d dry air gas constant, R_v water vapour gas constant, q_v specific content for water vapour, q_d specific content for dry air, $L_{vs}(T)$ latent heat of vaporisation ($T > 0^\circ\text{C}$) or sublimation ($T < 0^\circ\text{C}$), r_s^{li} mixing ratio for saturating water vapour for vaporisation ($T > 0^\circ\text{C}$) or sublimation ($T < 0^\circ\text{C}$), $e_{sat}(T)$ partial saturating pressure over liquid ($T > 0^\circ\text{C}$) or solid water ($T < 0^\circ\text{C}$), p pressure, and \widehat{Q} a weighting factor describing the ‘position’ of the buoyancy flux between unsaturated and fully saturated extremes.

Our approach for considering moisture in turbulent mixing requires S_{cc} and \widehat{Q} as inputs to the scheme. The dependence of \widehat{Q} on S_{cc} must be potentially non-linear due the non-Gaussian distribution of fluctuations. This effect is modelled by modulating the $\widehat{Q}(S_{cc})$ relationship through a skewness equivalent parameter - C_n , the whole according to data from Lewellen and Lewellen (2004). Once the nice results shown on Figure B1 are indeed converted into a parameterisation of the link between both quantities on the sole basis of the C_n value (directly computed from past diffusive fluxes), only one second relationship between S_{cc} and \widehat{Q} still needs to be specified. This may happen by further using the Lewellen and Lewellen (2004) framework and its mass-flux-type equivalence. But another kind of link may also be diagnosed by using vertical gradients of q_t and q_{sat} following the idea of Geleyn (1987) for computation of a ‘moist’ Richardson number Ri^* . In either case (and maybe in equivalent future proposals), the strength of this last closure step is to rely only on first order prognostic atmospheric variables and neither on information from earlier time-steps nor on variances or co-variances.

\widehat{Q} is also a crucial parameter in parameterising the vertical diffusion of $q_{l/i}$. This is based on the idea of Smith (1990) and further Gerard (2006) to obtain vertical fluxes of

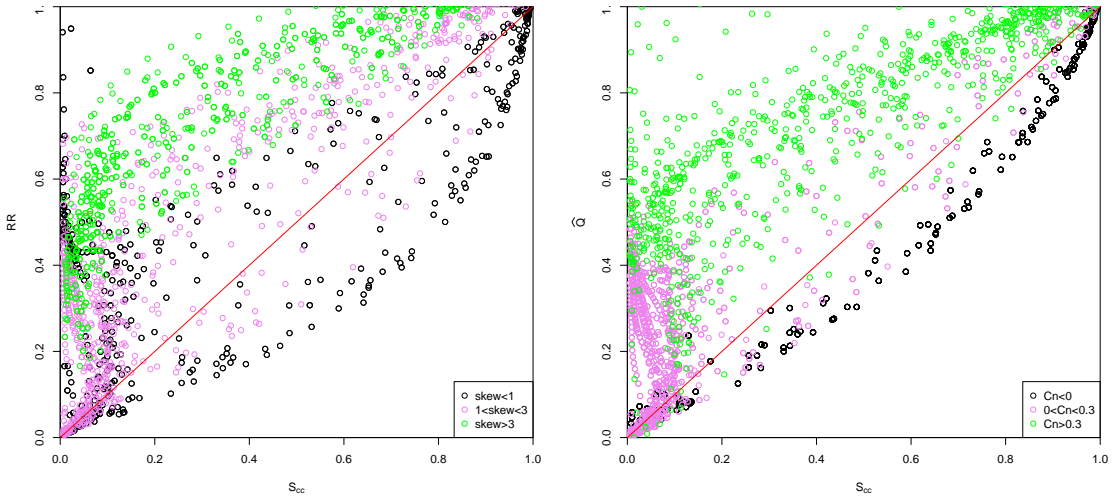


Figure B1: Comparison of $RR(S_{cc})$ (i.e. what would give the same buoyancy flux if ‘classically’ replacing simultaneously \widehat{Q} and S_{cc} in $M(S_{cc})$ for (B18) and (B19)) and $\widehat{Q}(S_{cc})$. The diagram on the left is the equivalent of Fig. 9 of Lewellen and Lewellen (2004), computed from the same LES data (courtesy of D. Lewellen) but with different thermodynamic hypotheses and using the reinterpretation of Marquet and Geleyn (2013). The colour scaling is based on skewness of the w subgrid-fluctuations. In the diagram on the right the colour scaling is based on C_n (a lower order term appearing in the analytical link between \widehat{Q} and $M(S_{cc})$). One clearly sees less dispersion and a more regular scaling in the second case, this validating the separation between both S_{cc} roles in (B18) and (B19)).

these quantities from fluxes of conserved quantities s_{sL} and q_t that are currently directly computed in the model, the whole according to the moist conservative scheme of Betts (1973).

B.3 Stability dependency functions’ framework

In TOUCANS we use our own framework of stability dependency functions, which are valid for all stability conditions and accounting of turbulence anisotropy in both momentum- and heat-related terms. This framework is based on Cheng et al. (2002) with modifications leading to the absence of critical gradient Richardson number in the system.

In this framework χ_3 , ϕ_3 , and ϕ_Q are expressed as functions of flux Richardson number:

$$\phi_3(Ri_f) = \frac{1 - \frac{Ri_f}{P}}{1 - Ri_f}, \quad (\text{B23})$$

$$\chi_3(Ri_f) = \frac{1 - \frac{Ri_f}{R}}{1 - Ri_f}, \quad (\text{B24})$$

$$\phi_Q(Ri_f) = \frac{1 - \frac{Ri_f}{Q}}{1 - Ri_f}, \quad (\text{B25})$$

$$\frac{Ri}{Ri_f} = \frac{P(R - Ri_f)}{C_3 R (P - Ri_f)}, \quad (\text{B26})$$

$$(\text{B27})$$

with R the variable describing the effect of the flow’s anisotropy on the turbulent momen-

tum exchange, Q the variable describing the effect of the flow's anisotropy on the turbulent heat exchange, and P the variable describing the joint effect of flow's anisotropy and TPE conversion on the turbulent heat exchange with : $\lim_{Ri \rightarrow \infty} P = Ri_{fc}$, and $Ri_{fc} = \lim_{Ri \rightarrow \infty} Ri_f$, critical flux-Richardson number.

The stability dependency function T_H is given by both stability parameters $Ri_{f,m}$ and $Ri_{f,s1}$:

$$T_H = \left\{ 2 C_3 S_{M,0} \lambda_5 \left[\phi_Q (Ri_{f,s1}) - \frac{\phi_Q (Ri_{f,m}) - \phi_3 (Ri_{f,m})}{2} \right] \right\}^{-1} \quad (\text{B28})$$

with $S_{M,0}$ and λ_5 closure coefficients.

Specific properties of this framework enable to emulate multiple turbulent schemes of different complexity (e.g. EFB turbulent scheme (Zilitinkevich et al. 2013), and QNSE turbulent scheme (Sukoriansky et al. 2005)). The hierarchy of the schemes is then given by the way the variables P , R and Q depend on stability (if all three variables are constants we get the simplest solution). For an overview of the basic stability dependency functions and of their quite differing shapes, see Figure B2.

The setting of the scheme is given by four free parameters: C_3 , O_λ , ν , and C_ϵ and, depending on the complexity of the emulated scheme, by additional stability dependent fittings of variables Q , R and/or P .

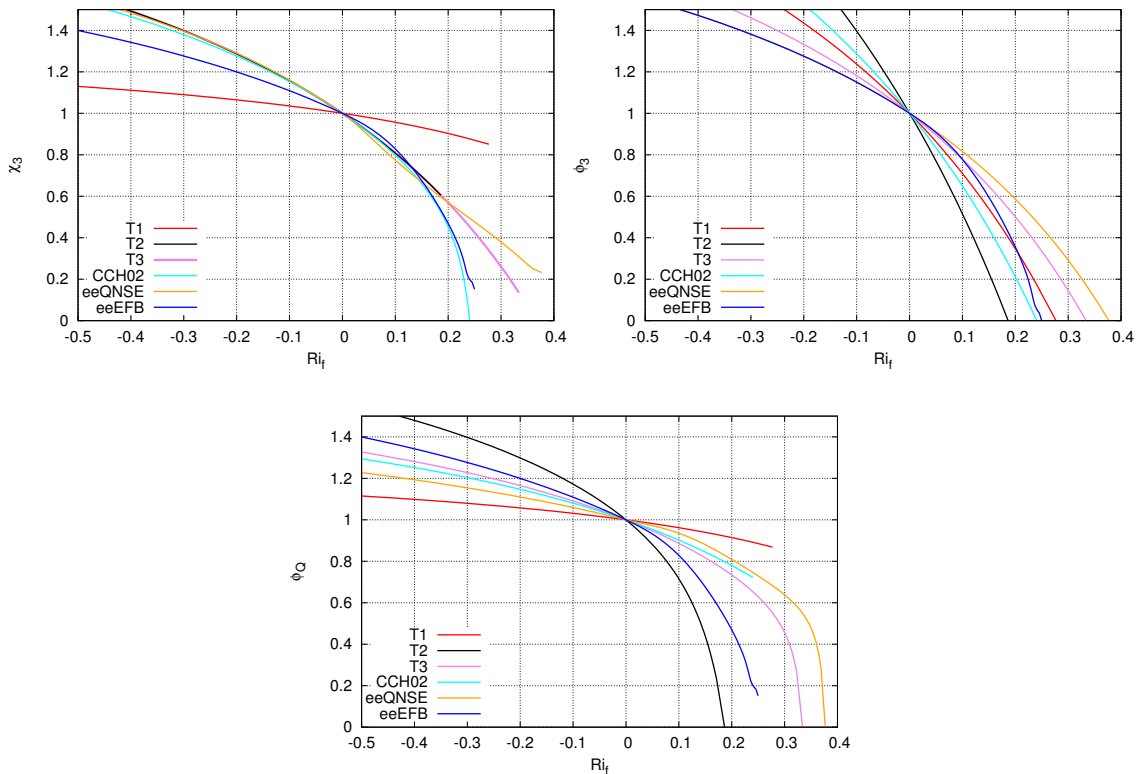


Figure B2: Stability dependency functions χ_3 (top left), ϕ_3 (top right), and ϕ_Q (bottom) for three variants of TOUCANS framework - T1, T2, and T3, Cheng et al. (2002) scheme - CCH02, emulation-extension (extension towards unstable stratification) of QNSE scheme - eeQNSE, and emulation-extension of EFB scheme - eeEFB. The most likely future choices are among T3, eeQNSE and eeEFB.

B.4 TOMs

TOMs parameterisation in TOUCANS offers a way of extending a conventional turbulence diffusion scheme with non-local mixing of heat and moisture as can be seen in (B6) and (B7).

If we express purely dry TOMs according to the proposal of Canuto et al. (2007):

$$\overline{w'^3} = -0.06\tau^2\overline{w'^2}\frac{g}{\theta}\frac{\partial\overline{w'\theta'}}{\partial z}, \quad (\text{B29})$$

$$\overline{w'\theta'^2} = -\tau\overline{w'\theta'}\frac{\partial\overline{w'\theta'}}{\partial z}, \quad (\text{B30})$$

$$\overline{w'^2\theta'} = -0.3\tau\overline{w'^2}\frac{\partial\overline{w'\theta'}}{\partial z}, \quad (\text{B31})$$

and extend the formalism to the moist case, relationships (B6) and (B7) can be rewritten so that the computation of turbulence tendencies leads to a solver with a tri-diagonal matrix. By using a two-pass computation with local diffusion as ‘first guess’ we are able to achieve stable and accurate computations, which are immune against singularities, and also computationally relatively cheap.

B.5 (Prognostic) length scale

The length scale in TOUCANS can be chosen quasi-independently from the stability dependency functions. Both mixing length from similarity laws (with notation l_m) and length scales computed from TKE (e.g. Bougeault and Lacarrere 1989) can be used due to the conversion relationship between them derived according to Redelsperger et al. (2001).

Since TKE-based length scales also depend on Brunt–Väisälä Frequency (BVF), their computation is generalised by using (moist) squared BVF (Vána et al. 2011) corresponding to the moist buoyancy term expressed in (B17).

The length scale computation is further enhanced by introduction of a prognostic approach (following Zilitinkevich et al. 2013, but replacing the time scale by the length scale as additional prognostic quantity), where a similar approach to the one of the evolution of TKE and TTE is used:

$$\frac{\partial L}{\partial t} = \frac{\partial}{\partial z} \left(K_{\text{TKE}} \frac{\partial L}{\partial z} \right) + \frac{2}{\tau} (\tilde{L} - L) \quad (\text{B32})$$

with \tilde{L} the usual ‘static’ length scale.

B.6 Time-step organisation

Taking into account all the above, the time-step for TOUCANS is organised in the following way.

First S_{cc} , Π^- , and $Ri_{f,s1}^-$ are computed from prognostic quantities and fluxes determined at the end of the previous time-step (from now on marked with index $-$). While S_{cc} is used to get weights E_{s_sL} and E_{qt,s_sL} (see (B18) and (B19)), Π^- , L^- , and e^- lead to computation of dissipation times scales τ , τ_{TTE} and exchange coefficients K_{TKE} , K_{TTE} . Weights E_{s_sL} and E_{qt,s_sL} and dissipation times scales τ , τ_{TTE} contribute to computation of the reference \tilde{e} (B10) and $\widetilde{\text{TTE}}$ (B11). The reference ‘moist’ mixing length \tilde{L} is obtained from Π^- and e^- .

The prognostic computation (without advection, which is performed by the dynamics of the model after the physics computations) of turbulent energies and mixing length is then executed (see (B8), (B9), and (B32)). The resulting turbulent energies (giving Π used for $Ri_{f,m}$) are, together with $Ri_{f,s1}$ and with the updated L value, used for computation of exchange coefficients K_M (B13) and K_H (B14) and terms that enter TOMs parameterisation.

Afterwards follows the actual computation of momentum, heat and moisture fluxes - $\overline{w'u'}$, $\overline{w'v'}$, $\overline{w'q'_t}$, $\overline{w's'_{sL}}$ - according to equations (B4)-(B7). The fluxes of s (dry static energy), q_v , q_l and q_i are then obtained back from fluxes of the conservative variables - q_t and s_{sL} .

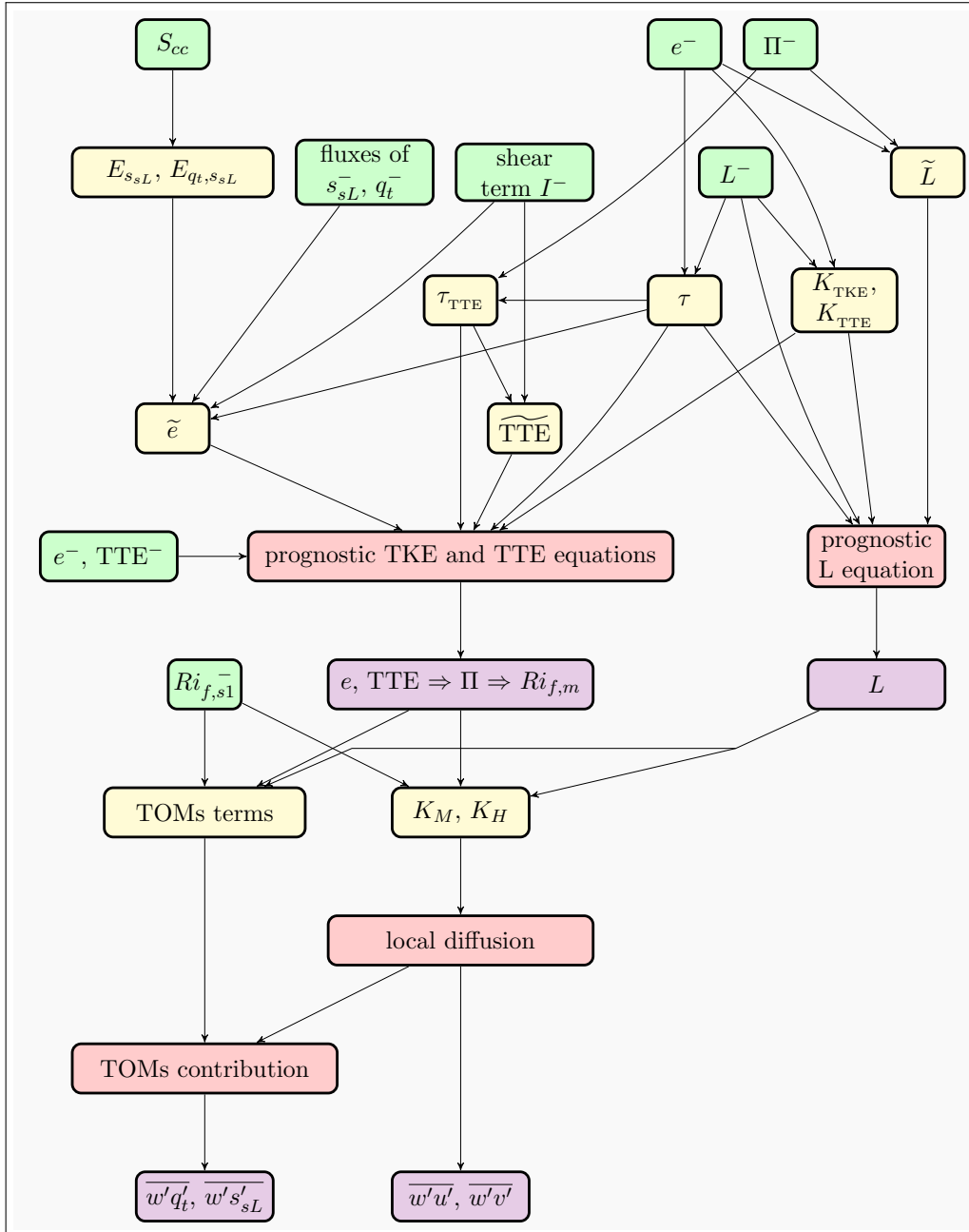


Figure B3: Main components of time-step organisation in TOUCANS.

Additional references

- Betts, A. K., 1973: Non-precipitating cumulus convection and its parameterization. *Quart. J. Roy. Meteor. Soc.*, **99** (419), 178–196.
- Bougeault, P. and P. Lacarrere, 1989: Parameterization of orography-induced turbulence in a mesobeta-scale model. *Mon. Wea. Rev.*, **117**, 1872–1890.
- Cheng, Y., V. Canuto, and A. Howard, 2002: An improved model for the turbulent PBL. *J. Atmos. Sci.*, **59**, 1550–1565.
- Geleyn, J.-F., 1987: Use of a modified Richardson number for parameterizing the effect of shallow convection. *J. Meteor. Soc. Japan, special NWP Symp. vol.*, 141–149.
- Gerard, L., 2006: The parametrisation of the turbulent diffusion fluxes in the presence of cloud ice and droplets: synthesis and application to Aladin. 6pp, URL www.rclace.eu/File/ALARO/DC.pdf.
- Smith, R. N. B., 1990: A scheme for predicting layer clouds and their water-content in a general-circulation model. *Quart. J. Roy. Meteor. Soc.*, **116**, 435–460.
- Váňa, F., I. Bašták, and J.-F. Geleyn, 2011: Turbulence length scale formulated as a function of moist Brunt–Väisälä frequency. *WGNE Blue Book*, chap. 4, 9–10.

Appendix C: The 3MT structure and some ideas about its concretisation, especially for the link with microphysics of convective-type clouds

J.-F. Geleyn

There are four core ideas used as pillars of the Modular, Multi-scale, Microphysics and Transport (3MT) scheme (Gerard et al. 2009):

- i. The ‘high-resolution limit’ accent which leads to have a clear orientation towards a full prognostic treatment of most key parameters of the scheme (Gerard and Geleyn 2005). Indeed, on top of the hydrometeors (all prognostic, except the graupel proportion in the falling ice-phase flux), there are prognostic equations for the updraft area fraction, for the in-plume updraft vertical velocity, for the downdraft area fraction and for the in-plume downdraft vertical velocity. Additionally, the cloudy detrained area fraction is treated as an historical variable (advected and updated at each time-step, though without having a specific independent prognostic equation). If one searches a more general way to justify such steps, it may be remarked that the microphysics bulk time scale (interval between condensation in clouds and falling water reaching the ground, roughly speaking) has the order of magnitude of the life-cycle of individual convective drafts. So both ‘memory’ aspects ought to be treated with similar care.
- ii. The M-T separation between microphysics and transport terms (Piriou et al. 2007) in the convective part of 3MT. There are two main advantages in doing this step, based on getting rid of the stationary cloud properties hypothesis. First, it allows incorporating any degree of complexity for the microphysical treatment of hydrometeors, independently of choices made in the convective parameterisation for the closure assumption and for the entrainment rate specification. In this respect, the microphysical scheme described later in this Appendix may be qualified as having ‘medium complexity’ (development of this package was strongly influenced by descriptions made in Lopez (2002), even if individual choices were somewhat differing in their details). Second, coupled with the existence of a prognostic treatment for the updraft area fraction, it leads to a core convective equations shape where updraft detrainment does not need to be parameterised anymore (this is also basically true for downdrafts). One may say that the detrainment becomes a diagnostic output of the convective part of 3MT computations, mainly controlled by detailed choices made when activating microphysical processes, with of course feedbacks at work from time-step to time-step.
- iii. The interaction between resolved condensation/evaporation, convective condensation, microphysics, downdraft organised evaporation/melting plus sedimentation relies on two basic principles: (a) in-cloud or precipitating water is unique, subject to the same physical laws whatever its origin; (b) the distinction between ‘resolved’ and ‘sub-grid’ condensation sources is arbitrary (Gerard 2007) since it depends on the model’s grid-size (there are ‘clouds’ or ‘drafts’ which will be seen as resolved for some small grid-meshes and as parameterised for bigger ones). Hence, in an attempt to avoid as much as possible the ‘grey zone syndromes’ of double-counting and/or double-void, only the sum of the ‘vapour \leftrightarrow condensates’ effects should matter and all other microphysical computations should ignore the hydrometeors’ origin. This

strategy is easy to apply in a local sense (i.e. in any well identified sub-grid area of a given model layer, see below). However it immediately raises another issue, namely that of the geometry along the vertical for the cloud scene and even its analogous for the precipitation covered areas. This must be treated by distinguishing sub-areas and making some overlap hypotheses (see for instance Shonk et al. 2010), something treated here with maximum generality and modularity, thanks to the special role dedicated to the APLMPHYS routine. The latter handles (1) the sedimentation of the three kinds of precipitating species, (2) the distinction for each layer between four sub-grid areas [cloudy area seeded from above by precipitations originating from cloud fractions higher-up, non-seeded cloudy area, seeded clear-air area, non-seeded clear-air area] as well as (3) the redistribution of fluxes' intensities and areas' extensions from each layer to the one just below, according to geometrical options (random-, maximum-random- and mixed-type for the overlap). APLMPHYS calls (several times per layer if appropriate) three routines wherefrom the actual physical processes are calculated (with as many grouped options of various origins as one wishes), respectively for auto-conversion-type processes, collection-type processes and phase-changes for falling hydrometeors.

- iv. The so-called ‘cascade’ way of updating thermodynamic prognostic variables both internally and externally of the main parameterisation algorithms. The principle applied here is to have on the one hand an approximated sequential treatment for the communication (in terms of the relevant quantities treated as prognostic by the whole model) between various 3MT steps. But, on the other hand, a parallel-type summation of all individual contributions to the resulting physical fluxes is used in order to get a global Green-Ostrogradsky-like computation for the interaction between physical and dynamical model tendencies, see Catry et al. (2007) for this latter aspect. Such a dual approach ensures at the same time an exact conservation of model invariants (energy, enthalpy and total water, for instance) and a communication of information between the various processes that does not need to wait for a change of time-step. This strategy acts as a complement to the above-mentioned prognostic orientation. The ‘internal’ update of the T and q_x equivalents is performed on the basis of simplified evolution equations: in a nutshell, the $C_p(q_x)$ parcel’s heat capacity and the $L_{v/s}(T)$ latent heats are kept at their values of the physics-time-step beginning, but this is true only for the internal updating process, of course. Protection against spurious negative values of the various water species is performed in parallel to cascade-linked updating steps.

Some notations (already used just above): all processes do modify prognostically handled values q_x for hydrometeors, with the following declination for ‘x’ (l = cloud liquid water, i = cloud solid water, r = rain, g = graupel, s = snow). However the thermodynamically transparent distinction between q_g and q_s is currently only diagnostic (i.e. performed at the microphysical package’s level, on the basis of separate sources and sinks). The sum $q_g + q_s$ thus builds a single advected variable. In short, one may say that the chosen simplification amounts to give to graupel thermodynamical properties of snow and mechanical properties of rain. A ‘prognostic graupel’ version of the ALARO microphysics is currently under development. Obviously, T is the temperature and q_v the q_x value for water vapour.

Given all the above, the sequence of events within the 3MT-concerned part of a ‘physics time-step’ can be roughly described as follows:

- Vertical diffusion (dry and moist turbulence, whatever the way they may be com-

bined) is computed. The results help upgrading T , q_v , q_l and q_i within the cascade. The obtained tendency of q_v is usually acting as part of the the convective closure forcing.

- The ‘resolved’ thermodynamic adjustment is performed in order to obtain: a stratiform cloud cover N_{str} , resolved condensation and evaporation rates as well as T , q_v , q_l and q_i upgrades within the cascade. It should be stressed that a provision must be made, inside the adjustment algorithm, for avoiding spurious re-evaporation of condensates of convective origin in an otherwise dry environment. The input parameter used to activate this ‘protection’ is the total (updraft plus detrained) convective area fraction N_{cv} , advected from the previous time-step. The way in which it acts depends on the internal characteristics of the thermodynamic adjustment process (here also various alternatives may be activated).
- The basic convective computations concerning updrafts are performed:
 - Computation of a plume ascent via budget equations and a rather complex prescription of entrainment, of buoyancy sorting (linked to memory of past precipitation evaporation rates) and of the Kershaw and Gregory (1997) parameterisation for the horizontal momentum transport, with horizontal pressure gradient effects taken into account.
 - Evolution of the in-plume vertical velocity via a full prognostic treatment (with memory thus), buoyancy, entrainment and friction being accounted for.
 - Closure assumption for determining a prognostic evolution of the vertically averaged ascent area fraction.
 - Mass-flux obtained from the product of both prognostic quantities.
 - Convective condensation rate obtained as product of the updraft mass-flux by a water vapour content vertical gradient, linked to the convective updraft plume. The delicate part is the choice of this gradient. At first sight one is tempted to use a gradient along the updraft ascent, classically obtained under moist adiabatic entraining conditions. But entrainment, which increases the said gradient, injects at the same time sub-saturated air inside the plume and this just compensates the gradient increase for the considered process. Hence the correct solution is to use the saturated water vapour vertical gradient within a fictitious local undiluted adiabatic ascent, calculated around full local properties of the basic entraining ascent. For computing the latter, a simplistic condensed water evaluation is needed. It is obtained by using the rough parameterisation proposed in Arakawa and Schubert (1974). The whole process writes, symbolically:

$$\left(\frac{\partial q_c}{\partial t}\right)_{\text{conv_cond}} = M_c \left(\frac{\partial q_{\text{sat}} ("h=\text{Cst}" + "\lambda_E \neq 0")}{\partial p}\right)_{"h=\text{Cst}" + "\lambda_E=0"} \quad (\text{C1})$$

where $q_c=q_l+q_i$ is the convective condensate amount (taken here for the whole grid-box), M_c the convective mass flux, q_{sat} the saturation water vapour amount (taken here in the plume), h the moist static energy and λ_E the entrainment rate.

- Computation of the transport terms for all prognostic variables (T , q_v , q_l , q_i , u and v).

- Diagnostic updating of N_{cv} , via a specific computation (with a life-time as tuning parameter) of the detrained area fraction.

It should be noted here that one aspect of the original M-T idea (i.e. that microphysics induced tendencies do all scale with respect to the mass-flux intensities) cannot be applied to the phenomena of melting and freezing around the treble-point temperature (i.e. only at a specific location in the vertical). Hence a very simplified microphysical scheme is applied to estimate those specific terms and all above-listed computations up to the mass-flux determination are iterated once.

- The subsequent cascade updating of q_l and q_i (on top of T and q_v of course) allows passing to the ‘local’ microphysical computations in-cloud condensation/evaporation rates that are the sums of those concerning stratiform (or resolved) clouds and of those concerning convective (or sub-grid) clouds. For the physics-time-step remaining part, no more distinction will exist between treatments of these two ‘sources’. As previously hinted at, this requires creating a microphysics-oriented cloud geometry along the vertical, which also combines both sources. This is performed on the basis of a specific combination of N_{str} and of N_{cv} at each model level.
- All local microphysical computations are then performed (see below the specific explanations about this important issue) and the ensuing cascade updating touches T , q_v , q_l , q_i , q_r and ‘ $q_g + q_s$ ’.
- The evaporation and melting of falling species induces a rate of cooling that will be used as part of the closure assumption for downdrafts.
- The basic computations concerning downdrafts (which may be caused by both convective and stratiform formation of precipitations before evaporation and/or melting, see above) are performed. They currently assume out-of-cloud but saturated conditions and they mirror updraft computations, but for the following differences:
 - One fixed uniform entrainment rate.
 - No buoyancy sorting but inclusion of a mechanism mimicking the flow divergence near the surface, in order to progressively obtain a zero mass-flux there.
 - No accounting of a detrained area fraction.
 - No need to iterate the M-T equations for the liquid \leftrightarrow ice phase changes, already fully accounted for in the scheme’s microphysics part.
- At the same time as applying the last updates against negative water amounts, one corrective step must be taken: the sedimentation computation performed earlier within the microphysics ‘package’ did consider precipitation rates which included falling species later diagnosed as ‘evaporated’ through the downdrafts’ action. A simple correction is indeed applied to compensate for this ‘false initial evaluation’. Unfortunately, short of iterating the whole microphysics calculation (which would be far too expensive), this step cannot be applied to other acting processes like collection, evaporation or melting-freezing of falling species. It is hoped that feedback loops acting from time-step to time-step will make up for this quasi-unavoidable slight inconsistency.

In summary, compared to other schemes of equivalent complexity, important 3MT features are the sequential organization, the M-T separation, the disappearance of the need

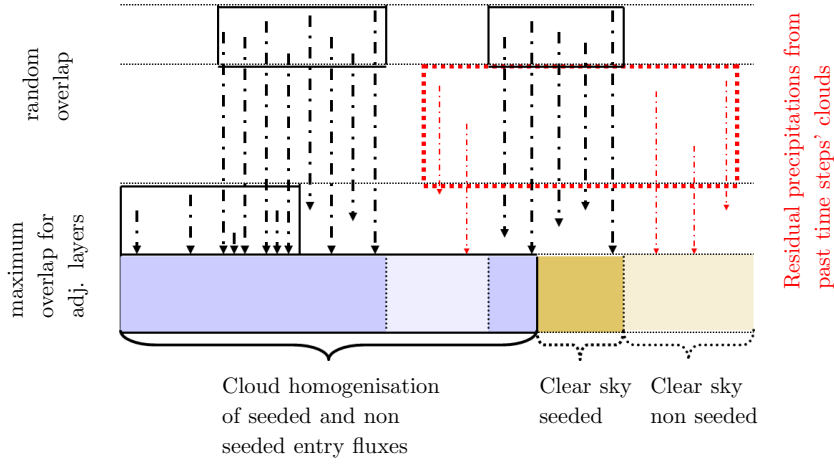


Figure C1: Schematic vertical geometry diagram for clouds and precipitations. Selected layer is colored, darker colors denote fractions seeded from clouds currently situated above. Red color denotes a previous cloud and its still falling precipitations. For each layer inside a downward vertical loop, the algorithm must recombine three outgoing sub-area-type fluxes into four incoming ones (each as input for one sub-area-specific computation of auto-conversion, collection and/or phase changes). The geometrical option is here the maximum-random overlap one.

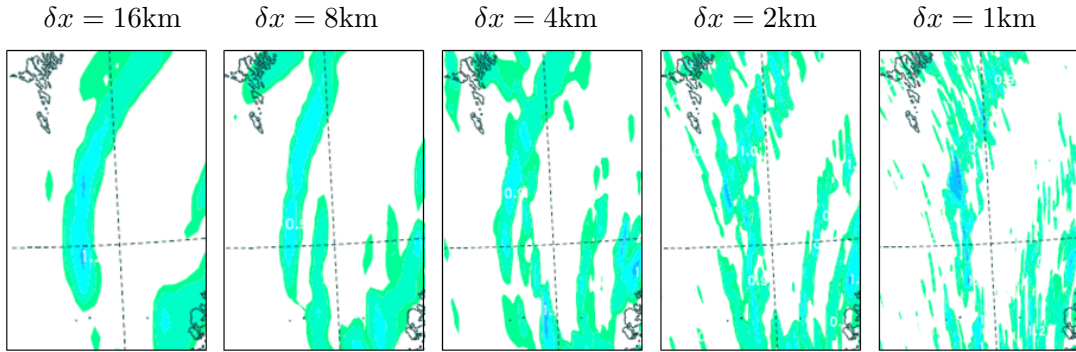


Figure C2: 1h precipitation amount forecast by the ALARO-0 baseline configuration including the 3MT scheme, for horizontal mesh-size 16km, 8km, 4km, 2km and 1km (from left to right). North Sea cold air outbreak case of the WGNE grey-zone intercomparison experiment, designed to explore the models' capacity to cope with partly resolved precipitating convection. This is a situation for which the 3MT scheme is targetted and it indeed delivers an unchanged basic solution with more and more details as resolution increases across the grey-zone. Forecast base 30 January 2010 at 12 UTC, forecast range +31h, sub-area results shown between the Feroes and Orkneys.

to parameterize convective detrainment rates, the use of prognostic variables in convective up- and downdrafts, the estimation, accumulation and decay of detrainment area fractions, the calculation of an updraft microphysical feedback, the protection of convective-origin condensates against re-evaporation, and the internal use of cloud geometry considerations in microphysics. Coming back to the 'philosophy' of all this development, one may say that

3MT is a way to do as if deep convection would be resolved but without needing to go to the scales where this is true for concrete applications (primary but not exclusive a grey-zone targeting). Links with microphysical considerations are numerous but in fact transparent to the degree of complexity of the used ‘package’. Practical care concerning the cloud and precipitation-covered areas’ geometry is essential (for a full discussion on this issue, see Turner 2011), but once this constraint is admitted, the full ‘APLMPHYS’ microphysics package can be considered as being both stand-alone and modular. It might thus even be used in other modelling frameworks. Figure C1 gives a graphical view on how the geometric aspects of clouds and precipitations are treated in APLMPHYS. Even if basic microphysics is only of medium sophistication and that progress of ACRANE2 and of TOUCANS have yet to be integrated in operational versions, the ALARO-0 configuration shows good multi-scale forecasting skills. For instance the 3MT quality with respect to its targeted scale-independency was evaluated for the Cold Air Outbreak grey-zone case proposed by (WMO)CAS/JSC WGNE, with mesh-sizes going down from 16km to 1km. An example of results for the challenge of localised and short interval precipitations is shown on Figure C2.

C.1 Some more details about the medium-complexity standard ALARO-0 micro-physical package

C.1.1 Parameterisation of auto-conversion-type processes

The Wegener-Bergeron-Findeisen (WBF) process is included in this item and is thus treated like an auto-conversion-type process from cloud liquid water to graupel (one intentionally by-passes the short transition through the wet crystals stage).

For pure auto-conversion, one uses the most simple but yet continuous (i.e. no absolute threshold below which no auto-conversion would occur) formulation, namely that of Sundqvist (1978). Two parameters control the process magnitude and speed, a cloud water critical amount and a time scale. Both are fixed values for liquid water converted to rain and temperature dependent values for solid water converted to snow.

The chosen parameterisation for WBF is that of Van der Hage (1995), a bit simplified and presented in a rescaled way showing both similarities and specific differences with respect to the parameterisations just described for basic auto-conversion. Important items are (a) the reference to a common ‘source’ with the cloud liquid water auto-conversion, (b) the fact that the WBF process is most active for comparable amounts of liquid and solid water condensates and (c) a critical quantity chosen as proportional to the geometric average of the liquid and solid ones within the basic auto-conversion processes.

The resulting analytical formulae are:

$$\left(\frac{dq_{l/i}}{dt}\right)_{\text{auto.conv}} = -\frac{q_{l/i}}{\tau_{l/i}} \left[1 - e^{-\frac{\pi}{4} \left(\frac{q_{l/i}}{q_i^{cr}}\right)^2}\right] \quad (\text{C2})$$

$$\tau_i(T) = \frac{\tau_i^0}{f_{ip}(T)}; \quad q_i^{cr}(T) = (q_i^{cr})_{\min} + [(q_i^{cr})_{\max} - (q_i^{cr})_{\min}] f_{ip}(T) \quad (\text{C3})$$

$$f_{ip}(T) = \min \left[1, e^{c_i^*(T-T_i)}\right] \quad (\text{C4})$$

$$\left(\frac{dq_l}{dt}\right)_{\text{WBF}} = -F_{\text{WBF}}^A \frac{q_l}{\tau_l} \frac{q_l q_i}{(q_l + q_i)^2} \left[1 - e^{-\frac{\pi}{4} \left(\frac{q_l q_i}{[F_{\text{WBF}}^B]^2 q_l^{cr} q_i^{cr}(T)}\right)}\right] \quad (\text{C5})$$

where τ represents the time scales, q^{cr} the critical amounts of cloud water and T_t the treble point temperature. Note that c_t^* is a temperature scaling, common here to all ice-phase linked temperature dependencies (there are five such dependencies proposed in Lopez (2002) but they only differ by about +/- 10% from a ‘consensus’ value, chosen here as unique, for the sake of computing efficiency).

C.1.2 Parameterisation of collection processes

One starts with the ‘pivot’ problem of cloud liquid water collection by rain. Alike in Lopez (2002), the principle is that of precipitation scanned volume times density of the collected specie, the whole being multiplied by a collection basic efficiency factor (0.2). The scanned volume computation is done on the basis of a Marshall and Palmer (1948) distribution law and of the Kessler (1969) double Γ -function algorithm. Extensions to the other five cases are based on the following principles:

- i. graupel and snow are joined when computing absolute dependency with respect to the precipitation flux but otherwise separated (via a proportionality factor to each flux), while graupel is assumed to have the collection efficiency of rain;
- ii. the temperature dependency for the capacity of catching ice-crystals is such that colder conditions favour smaller crystals, more likely to escape collection;
- iii. the temperature dependency of snowflakes capacity to catch cloud particles is exactly the opposite, since smaller flakes have a bigger surface to volume ratio.
- iv. Finally the value of the overall multiplying constant at 0°C for the snow case does incorporate all differences (with respect to the ‘pivot’ case) mentioned in Lopez (2002): twice smaller basic efficiency factor, far bigger intrinsic surface to volume ratio, a four time smaller ‘intercept value’ N_0 in the Marshall-Palmer formula. All included, this gives here about four times more collection efficiency for snow than for rain at 0°C.

The resulting analytical formulae are:

$$\left(\frac{dq_l}{dt}\right)_R^{\text{coll}} = -C_E^r R^{\frac{4}{5}} q_l \quad (\text{C6})$$

$$\left(\frac{dq_i}{dt}\right)_R^{\text{coll}} = -C_E^r R^{\frac{4}{5}} q_i f_{ip}(T) \quad (\text{C7})$$

$$\left(\frac{dq_l}{dt}\right)_G^{\text{coll}} = -C_E^r G (S + G)^{-\frac{1}{5}} q_l \quad (\text{C8})$$

$$\left(\frac{dq_i}{dt}\right)_G^{\text{coll}} = -C_E^r G (S + G)^{-\frac{1}{5}} q_i f_{ip}(T) \quad (\text{C9})$$

$$\left(\frac{dq_l}{dt}\right)_S^{\text{coll}} = -C_E^s S (S + G)^{-\frac{1}{5}} \frac{q_l}{f_{ip}(T)} \quad (\text{C10})$$

$$\left(\frac{dq_i}{dt}\right)_S^{\text{coll}} = -C_E^s S (S + G)^{-\frac{1}{5}} q_i \quad (\text{C11})$$

where R , G and S represent respectively the rain, graupel and snow precipitation fluxes.

C.1.3 Parameterisation of falling species phase changes

Evaporation

All three precipitating species do evaporate in ‘unsaturated clear air patches’. This formulation is preferred to that of ‘sub-cloud layers’, since falling species having yet to reach the ground at previous model time-steps may very well be above any cloud layer in the current time-step. And in this case they must still be subject to evaporation (and to melting/freezing, of course). The concrete algorithm prevents saturation overshoots.

Computation for the rain evaporation process closely follows the Kessler (1969) proposal on the basis of the Marshall and Palmer (1948) law. Starting from the famous $N(D) = N_0.exp(-\lambda D)$ formula, two Γ -function-containing integrals are computed, one for the rainfall rate and one for the rain-fall rate change via evaporation. Eliminating λ between the two equations, rounding the R exponent from 0.4521 to 0.5 (through a retuning of the formula for individual drops’ evaporation rates) and converting (in standard atmosphere tropospheric conditions) all three vertical dependencies into a single one concerning p (with an exponent -2.038 also rounded to -2.) delivers the formula below.

For the extension to graupel and snow, it is assumed that changes in the fall-speed would induce two opposite consequences: worse ventilation but longer residence time in a given model layer (or twice the opposite). Hence, for lack of better knowledge of these dependencies, after some trials, it was decided to leave the basic formula untouched when changing species. Snow and graupel are just treated together since they imply a differing computation of the target wet-bulb point from that for rain.

Melting of falling snow and graupel

Concerning falling snow and graupel, melting is fully parameterised, with a formula which is smoother than a yes/no one. The computation follows here also the Kessler (1969) as well as Marshall and Palmer (1948) options. Simplifications are the same as for evaporation of rain in clear air patches and the ratio between both model constants is simply $2\gamma C_{pd}/(\Delta L_f)$ where γ is the molecular diffusivity of heat, Δ the one of water vapour, C_{pd} the specific heat constant for dry air and L_f the latent heat of freezing. The proportion between snow and graupel fluxes is preserved during this process. One avoids undershoots in case of temperatures above but close to 0°C.

Freezing of falling rain

The computation exactly follows the one for melting of falling precipitations. But this ‘symmetric’ (re-)freezing process is considered far less efficient, with a tuning constant taken eighty times smaller. One avoids overshoots in case of temperatures below but close to 0°C. The resulting precipitating specie is graupel.

The resulting analytical formulae are thus:

$$\frac{d\sqrt{R}}{d(1/p)} = \frac{1}{2\sqrt{S+G}} \frac{dS}{d(1/p)} = \frac{1}{2\sqrt{S+G}} \frac{dG}{d(1/p)} = F_{\text{evap}}(q_w - q_v) \quad (\text{C12})$$

$$\frac{m_i}{m_s} \frac{dm_s}{d(1/p)} = \frac{m_i}{m_g} \frac{dm_g}{d(1/p)} = \frac{F_{\text{melt}}(T - T_t)}{\sqrt{S+G}}; \quad \frac{dm_i}{d(1/p)} = \frac{F_{\text{freez}}(T - T_t)}{\sqrt{R}} \quad (\text{C13})$$

where p is the pressure, q_w the wet-bulb water vapour amount (preferred to q_{sat} since this substitution implicitly accounts for the change of temperature induced by evaporation), m_s and m_g ($m_i = m_s + m_g$) the respective snow and graupel proportions of the total precipitation flux.

C.1.4 Parameterization of sedimentation

Precipitation sedimentation is computed according to the PDF-based method described in Geleyn et al. (2008), in its ‘exponential decay version’. The reader is referred to this paper for all details about methodology and resulting algorithmic choices. The other choice made in ALARO is to parameterise dispersion of falling species. This first requires knowing the fall speeds dependency on falling species’ amounts, more precisely obtaining a mean fall-speed for rain -and graupel- on the one side and one for snow on the other side. This is performed by a method very similar to that of Lopez (2002) which results are also used in the above-mentioned computations for collection and phase changes. For rain, the method follows closely that of Appendix B of Lopez (2002). But the dependency on air density and the formula’s final exponent (1/5 in the case of Lopez) differ owing to slightly different choices for Marshall-Palmer-type formulae. For the extension to snow, the fall-speeds’ ratio is exactly that of Lopez at 0°C (snow then falls about four times slower than rain) and it similarly increases for colder temperatures.

The resulting analytical formulae are:

$$\bar{w}^r = \Omega^r \left(\frac{R}{\rho^4} \right)^{\frac{1}{6}} ; \quad \bar{w}^g = \Omega^r \left(\frac{S + G}{\rho^4} \right)^{\frac{1}{6}} ; \quad \bar{w}^s = \Omega^s f_{ip}(T) \left(\frac{S + G}{\rho^4} \right)^{\frac{1}{6}} \quad (\text{C14})$$

where w stands for the various fall-speeds and ρ is the air density.

Additional references

- Arakawa, A. and W. Schubert, 1974: Interaction of a cumulus cloud ensemble with the large scale environment, Part I. *J. Atmos. Sci.*, **31**, 674–701.
- Gerard, L., 2007: An integrated package for subgrid convection, clouds and precipitation compatible with the meso-gamma scales. *Quart. J. Roy. Meteor. Soc.*, **133**, 711–730.
- Kershaw, R. and D. Gregory, 1997: Parameterization of momentum transport by convection. I: Theory and cloud modelling results. *Quart. J. Roy. Meteor. Soc.*, **123**, 1133–1151.
- Kessler, E., 1969: On the distribution and continuity of water substance in atmospheric circulations. *Meteorol. Monographs*, **10**, American Meteorological Society, Boston, USA.
- Marshall, J. S. and W. M. K. Palmer, 1948: The distribution of raindrops with size. *J. Meteorol.*, **5**, 165–166.
- Shonk, J., R. Hogan, J. Edwards, and G. Mace, 2010: Effect of improving representation of horizontal and vertical cloud structure on the Earth’s global radiation budget. Part I: Review and parametrization. *Quart. J. Roy. Meteor. Soc.*, **136**, 1191–1204.
- Sundqvist, H., 1978: A parameterisation scheme for non-convective condensation including prediction of cloud water content. *Quart. J. Roy. Meteor. Soc.*, **104**, 677–690.
- Turner, S., 2011: Nouvelle paramétrisation sous-maille et sous-nuageuse des précipitations. Ph.D. thesis, Paul Sabatier University, Toulouse, France.
- Van der Hage, J., 1995: A parametrization of the Wegener-Bergeron-Findeisen effect. *Atmos. Res.*, **39**, 201–214.

Appendix D: Anticipated evolutions within ALARO-1 towards a unique description of ‘cloudiness’

J.-F. Geleyn & L. Bengtsson - October 10, 2012

This note describes the anticipated changes needed within the model physics, in order to go from ALARO-0 to ALARO-1. The goal in ALARO-1 is to have physics, especially for clouds and precipitations, which is described in a unified way.

D.1 Thermodynamic-type ‘non-prognostic’ computations

Present situation

On the basis of raw, level-by-level, previous basic computations for T_w , q_w , q_{sat} , etc., the thermodynamic adjustment is done in ALARO-0 in two parts. At the start of the sequence, the sub-routine ACNEBCOND is called to compute (at each layer in the vertical):

- temperature-dependent proportion of ice phase water in the clouds F_{ice} .
- target saturation value (with the option to compute either q_w or q_{sat}).
- tuned critical relative humidity H_{uc} .
- final so-called ‘stratiform’ cloud-cover N_{str} .

Two remarks are here of interest:

- i. the computation uses as input the so-called ‘deep convective’ cloud-cover N_{cv} , brought in and advected from the previous model time-step, and this in order to ‘protect’ the convectively detrained condensates during past time-steps from a too quick re-evaporation;
- ii. owing to the ‘cascade spirit’, the four quantities described above shouldn’t have to be upgraded until the end of the ‘adjustment step’; this is true for the first three of them but rather doubtful for stratiform cloud-cover; it was nevertheless decided that it is important to use the same stratiform cloud-cover for turbulence, deep convection and radiation, even though there can be a contradiction with resolved condensation.

The second part of the thermodynamic adjustment is called after the turbulent diffusion computations. In this step the upgraded input variables (T and q_v) are adjusted due to latent heating/cooling and drying/moistening in the condensation computation step, done in the sub-routine ACCDEV. It was foreseen that the other input variables q_l and q_i should also be modified by the turbulent diffusion step of ALARO (including indeed the related parameterisation of shallow convection) and in an amount driven by the values of N_{str} . But this never worked correctly and was therefore left aside, making the case for the ACNEBCOND vs. ACCDEV split questionable.

Foreseen evolution

There should be an important evolution of this part, considering two important aspects.

- First, one wishes to abandon the idea that the radiative cloud characteristics should be computed in a purely diagnostic manner for their resolved part.

- Second, the introduction of the TOUCANS turbulent scheme will most probably require an initial computation of a so-called ‘shallow convection cloud-cover’ S_{cc} . This should be done independently of any subsequent computations within the physical time-step, even if the value may be strongly dependent on information from the previous model time-step. Furthermore, this new quantity shall be defined on the model’s half levels, in conformity with the vertical exchange role of shallow convection.

Currently, the equivalent of S_{cc} is computed internally (and in fact implicitly) in the turbulence-diffusion part done by the so-called ‘p-TKE’ scheme. Therefore, two changes in the present ACNEBCOND computations are foreseen:

- The ‘protection’ of the convective condensates will include shallow convection, such as using $N_{\text{nstr}} = N_{cv} + S_{cc} - N_{cv} \cdot S_{cc}$, contrary to the previous scheme where the protection was based on N_{cv} alone. S_{cc} will have to be first vertically averaged for that particular purpose.
- The ‘adjusted’ values of q_l and q_i corresponding to N_{str} will be produced in ACNEBCOND a first time (for input to the radiative computations). This requires the call to an algorithm similar to the one currently used in ACCDEV. The reason to keep a separation between stratiform cloud-cover computations and the thermodynamic adjustment thus becomes more and more artificial. A full merge of the two sub-routines can hence seriously be envisaged. But this should be done in preserving their general-purpose character with respect to ARPEGE- and RK-scheme-solutions.

It should be noticed here that, when implementing 3MT in the ARPEGE model, similar steps have been rather successfully attempted. There was a need for some retuning, since the basic parameterisations are different in ALARO and ARPEGE, and there is no doubt that it should also be the case in ALARO-1.

D.2 Radiative fluxes’ computations

Present situation

The diagnostic aspect of the radiative cloudiness requires a distinction, at each level in the atmosphere, between a so-called ‘resolved’ N_{res} part and its deep convective N_{cv} counterpart. This diagnostic aspect is only used for the forecasters, and does not change the model time-evolution. The actual radiative code sees only their combination $N_{\text{rad}} = N_{\text{res}} + N_{cv} - N_{\text{res}} \cdot N_{cv}$ and the associated pair of q_l and q_i values ($q_c = q_l + q_i$ being the condensed water for radiative computations).

The current algorithm is very complex but it relies on one relatively simple diagnostic formula proposed (on the basis of atmospheric measurements) by Xu and Randall, which gives a generic N from q_v , q_c and q_w , namely $N = (q_v/q_w)^{0.25} \cdot (1 - \exp(-\alpha \cdot q_c / (q_w - q_v)^{0.5}))$. So q_c is computed in a purely diagnostic way for the resolved part. The above formula is inverted in parallel using N_{cv} , and giving a complementary amount of deep convective condensate. This delivers the radiative q_l and q_i , after summation and with the help of F_{ice} , as well as it produces N_{rad} , from which N_{res} can eventually be inferred. In case of temperature inversions, a rather heuristic modification of the computation is done so that its diagnostic part should describe shallow convective clouds when relevant. But this has in fact nothing to do with the implicit S_{cc} value of p-TKE.

It should be noted here that the Xu-Randall formula, simplified by the replacement of $\exp(-x)$ by $1/(1+x)$, and complemented by $q_v = q_w(H_{uc}(1-N) + N)$ is the basis for the

already mentioned ALARO thermodynamic adjustment computations, ‘protection’ (made under the hypothesis of equal ‘local intensive’ values of q_c in all parts) also accounted for.

Foreseen evolution

Hopefully the process computations of ALARO-1 (deep convection, shallow convection and ‘protected’ thermodynamic adjustment) should be realistic enough to allow the removal of the diagnostic computation of a ‘resolved q_c ’. One hopes that the non-convective cloud cover $N_{\text{res}} = N_{\text{str}} + S_{cc} - N_{\text{str}} \cdot S_{cc}$ (S_{cc} vertically averaged here also) and the above-mentioned preservation of the condensed water horizontal homogeneity within the grid-mesh will deliver correct inputs for the radiation part. There will however be the additional need to treat some extreme cases (e.g. $N_{\text{str}} = 0$ and $N_{\text{nstr}} > 0$ that delivers no hint of the q_c value, etc.). As a remark, internal cloud overlap considerations for ACRANEB calculations are not at stake here, even if being important for the model’s results.

D.3 Turbulence and shallow convection computation of diffusion fluxes

Present situation

It has already been described in its absolute simplicity (no direct influence on the radiative part, no input-output on S_{cc} and zero turbulent fluxes of q_l and q_i).

Foreseen evolution

With the arrival of TOUCANS things will radically evolve. There will be an explicit value of S_{cc} , either computed in stand-alone mode or diagnosed on the basis of the earlier implicit method of p-TKE, but in both cases available before the call to ACNEBCOND (or to the combined ACNEBCOND/ACCDEV sub-routine). The prognostic condensates q_l and q_i will be diffused alike T and q_v (with an intensity related to the values of S_{cc} , as a more logical choice and a more appropriate vertical staggering than in the previous case). The hope is that this will help preparing, together with the updated computations of stratiform condensation, a coherent picture of clouds and condensates for the microphysical treatment. This should also be true, a bit more indirectly, for the radiative computations at the next time-step.

D.4 ‘Resolved’ condensation-evaporation amounts from the thermodynamic adjustment

Present situation

Nearly all was already explained. The subroutine ACCDEV takes the four fields, N_{str} , H_{uc} , q_w/q_{sat} and F_{ice} , computed by the sub-routine ACNEBCOND, as input together with the T and q_v fields, after the latter have been updated by the turbulent and shallow convection vertical diffusion. This delivers condensation-evaporation local tendencies (both possibilities are open since clouds may well re-evaporate) and only that. The subsequent microphysical use of these quantities will not be discussed much in this note, but of course still mentioned, see below.

Foreseen evolution

Logically, the relevant sequence of initial computations, currently done around ACNEBCOND (basic thermodynamics, thermodynamic equilibrium cloudiness in ‘protected’

mode), will be done again and merged together with the computations presently done in the sub-routine ACCDEV, delivering an updated value N_{str}^* , in addition to the condensation-evaporation local tendencies. Whether this will happen at unchanged sub-routines (with internal logical switches differing between the two calls of ACNEBCOND) or by the already mentioned possible merge is still to be decided. But the associated choice has no impact on the cloudiness issues treated in the present note.

D.5 Deep convective condensation and updraft transport

Present situation

Concerning the matter of cloudiness, this part delivers a deep convective cloud-cover N_{cv} . It also produces convective updraft condensation local tendencies (re-evaporation is not allowed at such a stage), which will be added to the ‘resolved’ corresponding output, before entering the single occurrence of microphysical cloud-precipitation computations. The vertical transport part of the convective updraft algorithm delivers fluxes for the same variables as the turbulent diffusion, including q_l and q_i . But this transport, although accounted for the budget of the variables at the end of the time-step, has no direct impact on cloudiness aspects.

Foreseen evolution

There is no need for evolution here, except a possible retuning of the amount of deep convective cloud-cover.

D.6 Various microphysical computations (apart from cloud creation or dissipation)

Present situation

The ‘clouds’ used in this part of the computations (in the general-purpose sub-routine APLMPHYS) play a key role for the geometric aspects governing the local intensity of cloud or clear-air processes and their influences along the vertical, when precipitating species go down from one layer to the next. But since they are considered as ‘joint’ between stratiform and deep convective considerations, their amount is produced by a complex formula combining the inputs N_{str}^* and N_{cv} . The resulting rather heuristic values N_{mp} will not be further re-used beyond this microphysical part of the physical time-step.

Foreseen evolution

One may need a revisit of the above-mentioned formula for N_{mp} , once the increased role of vertical diffusion will come in together with TOUCANS, but this is about all (even if very important by their impact and likely to evolve significantly in the future, internal overlap considerations for APLMPHYS calculations are not at stake here).

D.7 Downdraft additional evaporation and transport

Present situation

The downdrafts of ALARO-0 are ‘external and just saturated’, meaning that they do not interact with the matters concerning cloudiness, except of course very indirectly through their contributions to the various budgets of prognostic variables.

Foreseen evolution

None, given the above.

D.8 Summary

- Non-stratiform = (Deep) Convective & Shallow Convective \Leftrightarrow Stratiform
 - Resolved = Stratiform & Shallow Convective \Leftrightarrow (Deep) Convective
 - Precipitating = (Deep) Convective & Stratiform \Leftrightarrow Shallow (non prec.) Convective
 - First Stratiform \Rightarrow Second Resolved-Stratiform \Rightarrow Resolved($t + \delta t$) [in principle]
 - Radiative = [Resolved \cup Deep Convective]
 - Microphysical = f{Resolved-Stratiform , (Deep) Convective}
-

